MINISTÉRIO DA CIÊNCIA E TECNOLOGIA
INSTITUTO DE PESQUISAS ESPACIAIS

AUTORIZAÇÃO PARA PUBLICAÇÃO
AUTHORIZATION FOR PUBLICATION

PALAVRAS CHAVES/KEY WORDS

AUTORES / AUTHORS

PHASE TRANSITIONS
TWO-DIMENSIONAL SYSTEMS
SUPERCONDUCTING ARRAYS

AUTORIZADA POR/AUTHORIZED BY

Marco Antonio Raupp
Director General

AUTOR RESPONSAVEL
RESPONSIBLE AUTHOR

Enzo Granato

DISTRIBUIÇÃO/DISTRIBUTION

- [ ] INTERNA / INTERNAL
- [x] EXTERNA / EXTERNAL
- [ ] RESTRITA / RESTRICTED

REVISADA POR / REVISED BY

Antonio F. da Silva

CDU/UDC

537.312.62

DATA / DATE

Dezembro, 1987

PUBLICAÇÃO Nº
PUBLICATION NO

INPE-4457-RPE/559

ORIGEM
ORIGIN

LAS

PROJETO
PROJECT

TÍTULO/TITLE

PHASE TRANSITIONS IN TWO-DIMENSIONAL SUPERCONDUCTING ARRAYS IN A TRANSVERSE MAGNETIC FIELD

Nº DE PAG.
NO OF PAGES

93

ULTIMA PAG.
LAST PAGE

92

VERSÃO
VERSION

Nº DE MAPAS
NO OF MAPS

AUTORES/AUTHORSHIP

Enzo Granato

RESUMO - NOTAS / ABSTRACT - NOTES

The critical behavior of an array with a half flux quanta per unit cell is analysed in detail using a coupled XY model representation based on a Landau-Ginszburg free energy. This representation also describes others systems, and the analysis is extended to these systems as well. The model is transformed into an equivalent electrodynamic representation and recursion relations for small vortex fugacities and Migdal recursion relations are derived. A semi-qualitative analysis involving vortices and strings is used to argue on the possibility of a first order phase transition. The analysis is extended to different models like the fully frustrated XY model with unequal ferromagnetic and antiferromagnetic bonds and an XY model with competing periodicities. A simplified model of a superconducting array with weak disorder is presented. The model is mapped into a Coulomb-gas of fractional charges pertubed by a quenched distribution of randon charges or dipoles for the two kinds of disorder considered. Recursion relations using the replica trick and the implications of the results for the experimental systems is discussed. The Josephson-junction arrays studied by Voss and Webb (1982) is analysed in some detail. We porpose an interpretation of the variation of the resistance minima observed by these authors by including the presence of two incommensurate fundamental areas and the effects of weak positional disorder in the model.

OBSERVAÇÕES / REMARKS

Thesis presented at the Physics Department of Brown University, May 1986, Providence, RI, USA.

PHASE TRANSITIONS IN TWO-DIMENSIONAL SUPERCONDUCTING ARRAYS IN A TRANSVERSE MAGNETIC FIELD

by

Enzo Granato

B.S., São Paulo University, Brazil, December 1978
M.S., Instituto the Pesquisas Espaciais, Brazil, April 1982

Thesis

Submitted in partial fulfillment of the requirements for the
Degree of Doctor of Philosophy
in the Department of Physics at Brown University

May 1986

This dissertation by Enzo Granato
is accepted in its present form by the
Department of Physics as satisfying the
dissertation requirement for the degree of
Doctor of Philosophy.

Date ....

Recommended to the Graduate Council

Date ....

Date ....

Approved by the Graduate Council

Date ....

VITA

Enzo Granato was born in Juiz de Fora, M.G., Brasil, on January 16, 1955. He recieved a B.S. degree in Physics from the Universidade de São Paulo in December 1978 and a M.S. degree from the Instituto de Pesquisas Espaciais in April 1982. He also recieved a M.S. degree from Brown University in 1984. He has been a physicist at Instituto de Pesquisas Espaciais since 1979. His publications during the graduate work include:

" Critical behavior of coupled XY models ", Phys. Rev. B 33, 4767 (1986) (with J.M. Kosterlitz);

" Frustrated XY model with unequal ferromagnetic and antiferromagnetic bonds ", J. Phys. C 19, L59 (1986) (with J.M. Kosterlitz);

" Quenched disorder in Josephson-junction arrays in a transverse magnetic field ", Phys. Rev. B 33, 6533 (1986) (with J.M. Kosterlitz);

" Resistance oscillations in a Josephson-junction array in a magnetic field " (1986), submitted for publication (with J.M. Kosterlitz).

ACKNOWLEDGEMENTS

I would like to express my sincere gratitude to my advisor Professor John Michael Kosterlitz, whose enthusiasm and scientific guidance throughout my thesis work was immensily appreciated.

I also thank the other members of the group: Professors Robert Pelcovits, Anthony Houghton and See-Chen Ying. I have also benefited from helpful discussions with Devaraj Sahu and Nick Read.

It is a pleasure to thank my several friends who made my stay at Brown more enjoyable. Among these I should mention: Philip Weir, Hyekyung Won, Piali De, Rodney Torii, Gunnar Eliasson, Anuradha Jagannathan, Fernando Seco, Michael Altman and Steven Tiersten.

My graduate work at Brown was only possible due to the financial support recieved from Conselho Nacional de Desenvolvimento Científico e Tecnológico (CNPq) and Instituto de Pesquisas Espaciais (INPE). I also thank all my friends from the research group in INPE. Without their necessary support and motivation I would never come to Brown.

Finally, I am deeply indebted to my wife Mara and daughter Daniela whose love and encouragement have made this work possible. This thesis is dedicated to them.

Abstract of " *Phase transitions in two-dimensional superconducting arrays in a transverse magnetic field* " by Enzo Granato, Ph.D., Brown University, May 1986.

In the last few years, a number of research groups have used artificially-structured superconductors in the form of large two-dimensional ordered arrays of superconducting grains in order to study the phase transitions in two-dimensional superconductors in its lattice version. In the presence of a perpendicular magnetic field, completely new behavior has been observed. Measurements by several groups reported a periodic variation of the resistance of the array as a function of the magnetic field with resistance minima at each integer value of the number of flux quanta per unit cell as well as secondary minima at half-integer values of this number.

We review the general properties of an ordered superconducting array, set up the model and discuss the approximations involved. The resistive behavior of the array at zero field is shown to be determined by the vortex-unbinding transition in the pure XY model. Some recent approaches to the finite-field case are also presented.

The critical behavior of an array with a half flux quanta per unit cell is analysed in detail using a coupled XY model representation based on a Landau-Ginszburg free energy. This representation also describes others systems, and the analysis is extended to these systems as well. The model is transformed into an equivalent electrodynamic representation and recursion relations for small vortex fugacities and Migdal recursion relations are derived. A semi-qualitative analysis involving vortices and strings is used to argue on the possibility of a first order phase transition. The analysis is extended to different models like the fully frustrated XY model with unequal ferromagnetic and antiferromagnetic bonds and an XY model with competing periodicities.

A simplified model of a superconducting array with weak disorder is presented. The

model is mapped into a Coulomb-gas of fractional charges perturbed by a quenched distribution of random charges or dipoles for the two kinds of disorder considered. Recursion relations using the replica trick and the implications of the results for the experimental systems is discussed.

The Josephson-junction arrays studied by Voss and Webb (1982) is analysed in some detail. We propose an interpretation of the variation of the resistance minima observed by these authors by including the presence of two incommensurate fundamental areas and the effects of weak positional disorder in the model.

CONTENTS

LIST OF FIGURES

Figure *page*

Chapter 1

INTRODUCTION

In response to the theoretical work by Kosterlitz and Thouless (1973) and Berezinskii (1970) on the vortex-unbinding mechanism in phase transitions in two-dimensional systems, a large amount of experimental and theoretical work has been devoted to the application of this theory to a variety of different physical systems ranging from two-dimensional superfluids to adsorbed systems. A useful review of these and other topics can be found in Kosterlitz and Thouless (1978) and Nelson (1984).

The common feature of the Hamiltonian for these systems is the existence of a continuous symmetry of the order parameter which allows "vortices" and "anti-vortices" as the topological elementary excitations. Despite rigorous proofs by Mermin and Wagner (1966) for the absence of long-range order, a phase transition at a finite temperature is possible, below which thermally excited vortex pairs appear only as bound vortex-antivortex pairs and above which single vortices and anti-vortices are present in thermodynamic equilibrium. Such a transition is only possible if the interaction energy between the vortices depends logarithmically on the distance. Because of this logarithmic dependence on the distance, the system of vortex excitations can also be viewed as a two-dimensional neutral Coulomb gas.

A renormalization-group approach has been developed by Kosterlitz (1974) in order to account for the effects of small vortex pairs on the interaction energy between vortex pairs with larger separations. When applied to two-dimensional neutral superfluids, Nelson and Kosterlitz (1977) have established a universal relation between the transition temperature and the superfluid density. Experiments have been reported that apparently confirm this prediction (Bishop and Reppy, 1978).

As first shown by Pearl (1965), in thin superconducting films, a vortex pair interacts logarithmically only up to a characteristic distance of order of the transverse penetration depth Λ_T for perpendicular magnetic fields. For larger separations the interaction energy falls off as the inverse of the separation distance. The finite range of the logarithmic interaction in the superconducting film would then destroy the transition.

However, as pointed out by Beasley, Mooij and Orlando (1979), in thin-film dirty superconductors with appreciable normal-state resistance, the transverse penetration depth Λ_T can be comparable with the sample size. So, for practical systems, thermally excited vortex pairs interact logarithmically.

Because of this, most experimental and theoretical work has been on high-resistance or granular superconductor films. These systems, however, are far from ideal and randomness and inhomogeneities make the detailed comparison of theory and experiment a difficult task. It is also not yet clear what effect microscopic randomness or inhomogeneity has on the vortex-unbinding transition.

In the last few years, a number of workers have turned their attention to artificially-structured superconductors. In particular, several research groups have constructed large two-dimensional arrays of superconducting weak links to study the two-dimensional superconductor problem in its lattice version. Lobb et al (1983) have worked out formulas relating uniform film quantities to array quantities. Voss and Webb (1982) have made use of arrays of Josephson-junctions which were constructed as a result of the IBM effort to produce identical junctions for use in a superconducting computer. It is clear that such arrays offer a useful experimental system for understanding the phase transition in two-dimensional superconductors since the effects of randomness can be minimized. In addition, it is also possible to study the effects of artificially introducing inhomogeneities. For example, Davidson and Tsuei (1981) have studied the effects of introducing inhomogeneities on a two-dimensional Josephson tunnel junction array using a laser to cut a number of connections between the superconducting grains.

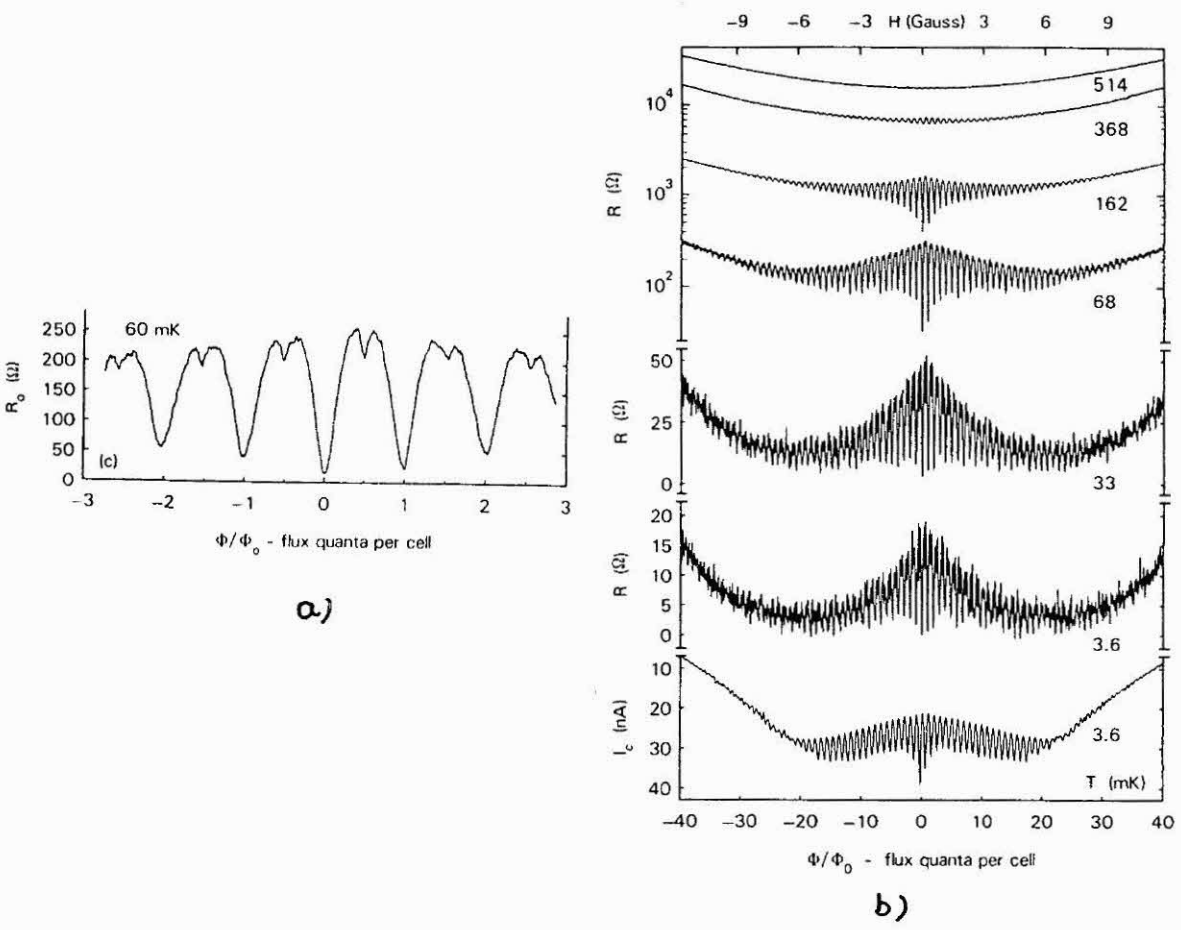

Figure 1.1 Resistive behavior of the IBM Josephson-junction arrays. Here Φ/Φ_o denotes the number of flux quanta Φ_o contained in the magnetic flux Φ threading a unit cell of the array. a) Resistive behavior at low fields; b) resistive behavior at larger fields and at various temperatures (Webb et al, 1983).

In the presence of a transverse magnetic field, completely new behavior has been observed. Early measurements by Voss and Webb (1982) reported a periodic variation of the resistance of the array as a function of the magnetic field, with a resistance minima at each integer value of the flux quanta per unit cell. Subsequently, Webb et al (1983) (Figure 1.1), Tinkham et al (1983) and Kimhi et al (1984) (Figure 1.2) have observed secondary minima at half-flux quantum per unit cell. Monte Carlo simulations by Teitel and Jayaprakash (1983a) of phase transitions in uniformly frustrated XY models, which are used to model these systems, are consistent with these observations and also indicate the existence of subsidiary minima at others rational values of the number of flux quanta.

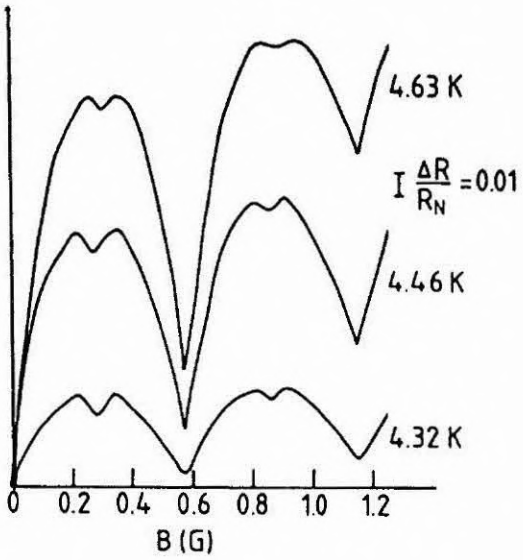

Figure 1.2 Resistive behavior of an array of weak-coupled grains. The array consists of Pb square grains arranged on a square lattice (Kimhi et al, 1984).

An immediate question that arises is the nature of the phase transitions at the various rational values of the number of flux quanta per unit cell and the existence or not of a phase transition at irrational values of this ratio. This has been the subject of intense work by several authors recently.

This thesis is the result of an investigation on the nature of the phase transition at simple rational values of the number of flux quanta per unit cell and on the effects of disorder on the resistive behavior of the array.

The thesis is organized as follows. In the following chapter, we review the general properties of an ordered superconducting array. We set up the model and discuss the approximations involved. Next the resistive behavior of the array at zero field is shown to be determined by the vortex-unbinding transition in the pure XY model. We then present the experimental results at finite field and briefly review some recent approaches to this problem. Finally we discuss in detail the role of the excitations in the fully frustrated case which corresponds to a half flux quantum per unit cell. This provides the motivation for the analysis of the subsequent chapter.

In Chapter 3, we analyse in detail the critical behavior of an array with a half flux quantum per plaquette using a coupled XY model representation based on a Landau-Ginzburg free energy. This representation also describes others systems, and we extend the analysis to these systems as well. The model is transformed into an equivalent electrodynamic representation and recursion relations for small vortex fugacities and Migdal recursion relations are derived. A semi-quantitative analysis involving vortices and strings is used to argue on the possibility of a weak first order transition. The analysis is extended to different models like the fully frustrated XY model with unequal ferromagnetic and antiferromagnetic bonds and an XY model with competing periodicities.

In Chapter 4, we present a simplified model of a superconducting array with weak disorder. The model is mapped into a Coulomb-gas of fractional charges perturbed by a quenched distribution of random charges or dipoles for the two kinds of disorder considered. Recursion relations using the replica trick are derived and the implications of the results for the experimental system is discussed.

In Chapter 5, we propose an interpretation of the variation of the resistance minima observed by Webb et al (1983) by modifying the simple model considered in Chapter 2 to include the presence of two incommensurate fundamental areas. We them combine the results of this analysis with the results of Chapter 4 to explain their experimental results.

Finally, Appendices A, B and C provide some of the details that were left out in the previous Chapters.

Chapter 2

TWO-DIMENSIONAL SUPERCONDUCTING ARRAYS

2.1 Introduction

Inhomogenous superconductors have attracted much attention in recent years; a useful review can be found in Gubser et al (1980) and Goldman and Wolf (1984). Typically, these materials are composed of two constituents, one is a superconductor while the other is a normal metal, an insulator or another superconductor with a lower transition temperature. Recent advances in microfabrication techniques, have made it possible to construct large arrays of superconducting grains (order of 10^6) in the form of ordered, two dimensional structures. The grains can be of various shapes (disks, asterisks, crosses and squares) with dimensions of order of μm. These arrays thus open the possibility of studying the properties of inhomogeneous superconductors in a controllable way.

Our main concern here is with two-dimensional arrays of superconducting grains embedded in a non-superconducting host and coupled together by Josephson tunneling, in the case of insulator, or proximity effect in the case of a normal metal host.

Superconducting wire networks also form an interesting system with similar properties to the arrays. Like the arrays, they can be prepared in a variety of forms by photolithographic techniques and other methods.

In this chapter we review the general properties of an ordered superconducting array with and without an external magnetic field present and briefly discuss some of the recent approaches to the problem. We also include a detailed analysis of the elementary excitations for the fully frustrated case which corresponds to a square or trangular array with a half

flux quanta per plaquette.

2.2 The model

A bulk superconductor is characterized by a complex order parameter $\Psi = |\Psi| e^{i\theta}$ where the magnitude $|\Psi|$ is in general temperature dependent and proportional to the Bardeen-Cooper-Shrieffer (BCS) energy gap of the superconductor.

When two superconductors are in close proximity, there is a term in the free energy which depends on the phase difference between them, i.e., (see for example Tinkham, 1975)

$$E = -J_{12} cos(\theta_1 - \theta_2) \tag{2.1}$$

The coupling energy is related to the maximum, or critical current I_{12} that can flow between the two superconductors by

$$J_{12} = \frac{h}{2e} I_{12} \tag{2.2}$$

where h and e are the fundamental constants.

For a weakly coupled array of superconducting grains the superconducting transition can occur in two stages. Around the transition temperature T_{co} of the grain, each separate grain will exhibit a smeared transition (due to finite-size effects) to a state where the modulus of the order parameter $|\Psi|$ builds up a non-zero value. Provided the Ginzburg-Landau coherence length ξ_{GL} of the bulk material comprising the grains is of the order of the grain size, the order parameter in each grain does not vary appreciably. If in addition, the effective coherence length of the array is of the order of the intergrain spacing, the grains will fluctuate independently. At a lower temperature T_c, the phases of the superconducting order parameter in the grains will lock due to the coupling and the system will become superconducting. This phase locking transition at zero magnetic field is isomorphic to the XY model phase transition (see Section 2.2).

Therefore, for temperatures below the bulk superconducting transition temperature and for weakly coupled grains, the Hamiltonian describing a two-dimensional superconducting

array can be generalized from (2.1) to

$$H = -J \sum_{<rr'>} \cos(\theta_r - \theta_{r'}) \tag{2.3}$$

where θ_r are the phases of the order parameter of the grains located at the site $\vec{r}$ of a lattice. In general J will be a function of temperature or the magnetic field (see Section 2.4), but we will assume it constant from now on.

Equation (2.3) makes the oversimplified assumption of "point grains". It also ignores the charging energy which arise from finite intergrain capacitance. This term should be added to (2.3) and it is of the form

$$H_c = -\frac{e^2}{4C} \sum_r (\frac{\partial}{\partial \theta_r})^2 \tag{2.4}$$

When (2.4) is added to the Hamiltonian (2.3) the problem is quite difficult and it is a matter not yet fully resolved (see for example José, 1984). In general, large charge energies , i.e., small capacitances tend to suppress phase coherence (Doniach, 1981). Charge energy is roughly associated with small grain sizes. We therefore assume here that the superconducting arrays to which (2.3) applies consist of grains that are simultaneously large enough so that charging effects can be ignored and sufficiently small so that the field dependence of the effective coupling is negligible (see Section 2.4).

In the presence of a perpendicular magnetic field, the phase difference in (2.1) is replaced by a "gauge-invariant" phase difference $\theta_r - \theta_{r'} - \frac{2\pi}{\Phi_o} \int_r^{r'} \vec{A} \cdot \vec{dl}$, where the extra term is just the line integral of the vector potential and $\Phi_o = \frac{hc}{2e}$. In consequence (2.3) is replaced by

$$H = -J \sum_{<rr'>} cos(\theta_r - \theta_{r'} - A_{rr'}) \tag{2.5}$$

where

$$A_{rr'} = \frac{2\pi}{\Phi_o} \int_r^{r'} \vec{A} \cdot \vec{dl} \tag{2.6}$$

Since $\vec{B} = \vec{\nabla} \times \vec{A}$, we must require the constraint

$$\sum_R A_{rr'} = 2\pi f \tag{2.7}$$

i.e., the directed sum of the $A_{rr'}$ (indicated here by the symbol $\sum_R$) around each plaquette with center at $\vec{R}$, is a constant, which is proportional to the magnetic field threading the plaquette in units of the magnetic flux quantum

$$2\pi f = \frac{2\pi HS}{\Phi_o} \tag{2.8}$$

where S is the area of the plaquette.

Throughout the following Sections we will assume that the $A_{rr'}$ are quenched in by the external field. This corresponds to taking the limit of very large London penetration depth for the array. In this limit the magnetic field penetrates the array homogeneously and there is no Meissner effect in the grains.

All equilibrium properties can be obtained from the knowledge of the partition function

$$Z = \left[\prod_r \int_0^{2\pi} d\theta_r\right] e^{-\frac{H}{kT}} \tag{2.9}$$

and the corresponding free energy $F = -k_B T \ln Z$.

It is easy to show that the Hamiltonian (2.5) is periodic in f with period 1, has a reflection symmetry about $f = 1/2$ in the interval $[0, 1]$ and is also invariant under the interchange $f \rightarrow -f$.

In experiments, however, the observed periodicity in f is seen to be modulated by an envelope function (see Figures 1.1 and 1.2). Teitel and Jayaprakash (1983a), have suggested that this effect can be accounted for within the model (2.5) by including an H dependence for the coupling J. This dependence is easy to undertand for proximity-coupled junctions. For junctions with an effective area $S' < S$, one expects $J(H)$ to have periodicity HS'/Φ_o, corresponding to every time an additional flux quantum threads the gap. Note however that for the kind of array used by Webb et al (1983), this effect is quite small since in this case the junction lies paralell to the field (see Chapter V).

The model defined by (2.5) belongs to a class of "uniformly frustrated XY models" where f is the frustration variable. Varying the external field then corresponds to varying the frustration in these models.

It might appear at first sight that Z and therefore the quantities calculated from it depend on the $A_{rr'}$ configurations since one only requires the constraint (2.7). Note however that under the gauge transformation $A_{rr'} \rightarrow A'_{rr'} + \Lambda_r - \Lambda_{r'}$, if we also perform a change of variables $\theta_r \rightarrow \theta_r - \Lambda_r$ the partition function (2.9) is now a function of $A'_{rr'}$. Therefore the partition function can only depend on gauge-invariant quantities such as (2.7). This implies that the models with the same f are equivalent.

The meaning of the frustration can perhaps be better understood by considering the so-called fully frustrated model, i.e., $f = 1/2$. Consider a square lattice array in a particular gauge in which $\vec{A} = Hx\hat{y}$ (Landau gauge), then (2.6) can be written as

$$A_{rr'} = 2\pi f \frac{x_r + x_{r'}}{2}(y_r - y_{r'}) \tag{2.10}$$

Direct substitution in (2.5) with $f = 1/2$ gives

$$H = -\sum_{<rr'>} J_{rr'} cos(\theta_r - \theta_{r'}) \tag{2.11}$$

where $J_{rr'} = J$ for horizontal bonds and $J_{rr'} = -J$ for alternating vertical bonds. The model defined by (2.11) has been studied by Villain (1975) in the context of the spin glass problem.

Note that because the product of the bond signs around a given plaquette is negative, the spins cannot simultaneously satisfy the ground state configuration (Figure 2.1). Figure 2.1b shows a non-frustrated plaquette. Note that the presence of negative bonds is not a sufficient condition for the frustration effect.

For the general case of (2.5), we look at the quantity $e^{i\sum_R A_{rr'}} = e^{2\pi fi}$ which is the analogue of the product of the bond signs in the previous example. If f is an integer the plaquette is not frustrated.

2.3 Zero-field behavior

We must pause now to briefly review the behavior of the superconducting array when no field is applied. This will provide the motivation and the background necessary for the discussion that follows.

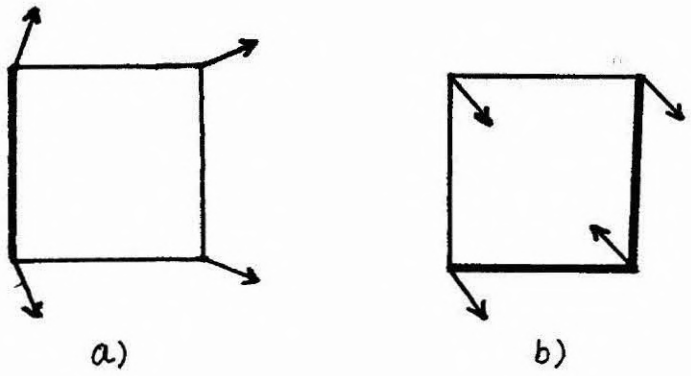

Figure 2.1 Frustation effect in a 2D XY model. Thick lines corresponds to antiferromagnetic bonds and thin lines to ferromagnetic bonds. a) frustrated plaquette; b) non-frustrated plaquette.

2.3.1 Vortex unbinding in the 2D XY model

Consider for the moment a generalized classical spin model given by the Hamiltonian

$$H = -J \sum_{<rr'>} \vec{S}_r \cdot \vec{S}_{r'} \tag{2.12}$$

where $\vec{S}_r$ are n component spins defined at the sites $\vec{r}$ of a d-dimensional lattice. If $n = 1$, we have the Ising model, $n = 2$ the planar (or XY) model and $n = 3$ the classical Heisenberg model. As mentioned before, the superconducting array defined by (2.3) is isomorphic to the XY model in $d = 2$ dimensions since when we parametrize the $\vec{S}_r$ by an angle θ_r as $\vec{S}_r = cos\theta_r \hat{x} + sin\theta_r \hat{y}$ we obtain directly (2.3).

In the study of the phase transitions associated with (2.12), it is crucial to distinguish the dimensionality of the spin n and the dimensionality d of the space. The existence of a conventional second-order phase transition in which an "order parameter" (for example the magnetization), develops below some critical temperature depends strongly in both n and d. For $n = 1$, there is a transition for $d = 2$, but not for $d = 1$. So the lower critical dimension is $d = 1$ for $n = 1$. For $n > 1$ the question is more complicated. The difference here is

that for $n > 1$, the model has a continuous rotational symmetry. It has been established by Mermin and Wagner (1966) that the global spin rotation symmetry of the ferromagnetic model (2.12), with $n \geq 2$ in two dimensions, can not be spontaneously broken at finite temperatures. This means that there is no possibility of conventional long-range order at nonzero temperature. The absence of long-range order however does not imply that there is no phase transition and a transition does in fact occur for $d = 2$, $n = 2$ although of peculiar type, in the sence that the magnetic susceptibility is infinity below T_c, but the average magnetization is zero (Kosterlitz and Thouless, 1973).

We shall concentrate now in the study of the phase transition for $n = 2$ and $d = 2$. Since we are interested in the low temperature behavior we expand the cosine in (2.12) as

$$H = -\frac{1}{2} \sum_{<rr'>} (\theta_r - \theta_{r'})^2 + constant \tag{2.13}$$

For fluctuations of wave length much larger then the lattice spacing, we can replace (2.13) by a continuum approximation

$$H = \frac{J}{2} \int (\nabla \theta_r)^2 d^2 \vec{r} \tag{2.14}$$

If finally we neglect the $\theta \rightarrow \theta + 2\pi n$ periodicity in θ and extend the integration from $-\infty$ to ∞, correlation functions can be calculated by a straighfoward gaussian integration. One then obtain

$$< e^{i(\theta_r - \theta_o)} > = |\vec{r}|^{-\eta} \tag{2.15}$$

where $\eta = \frac{k_B T}{2\pi J}$. This implies that there is no true long-range order but only a quasi-long-range order.

This is a rather unexpected behavior. Since there is no long-range order one should expect naively that the correlation (2.15) should decay like $e^{-r/\xi}$ with finite ξ as in a conventional paramagnetic phase. Here however we have a power-law behavior. On the other hand, power-law behavior is a characteristic of a critical point . In this case η is usually a universal value for a particular class of models. So we can view (2.15) as a line

of fixed points, one for each temperature. Eventually, at some higher temperature this power-law behavior must turn into a exponential behavior and the line of fixed points must terminate at some finite temperature.

The nature of the phase transition for the XY model was explained by Kosterlitz and Thouless (1973) who introduced vortex and antivortex as the missing excitations that were neglected in the spin wave appoximation (2.13). The inclusion of these excitations cause a phase transition at finite T_C. Because θ_r is a multivalued function, a contour integral of the type

$$\oint \vec{\nabla}\theta \cdot \vec{dl} = 2\pi n \tag{2.16}$$

has in general $n \neq 0$. In this case any countour must enclose at least one singularity, known as a vortex (see Figure 2.2).

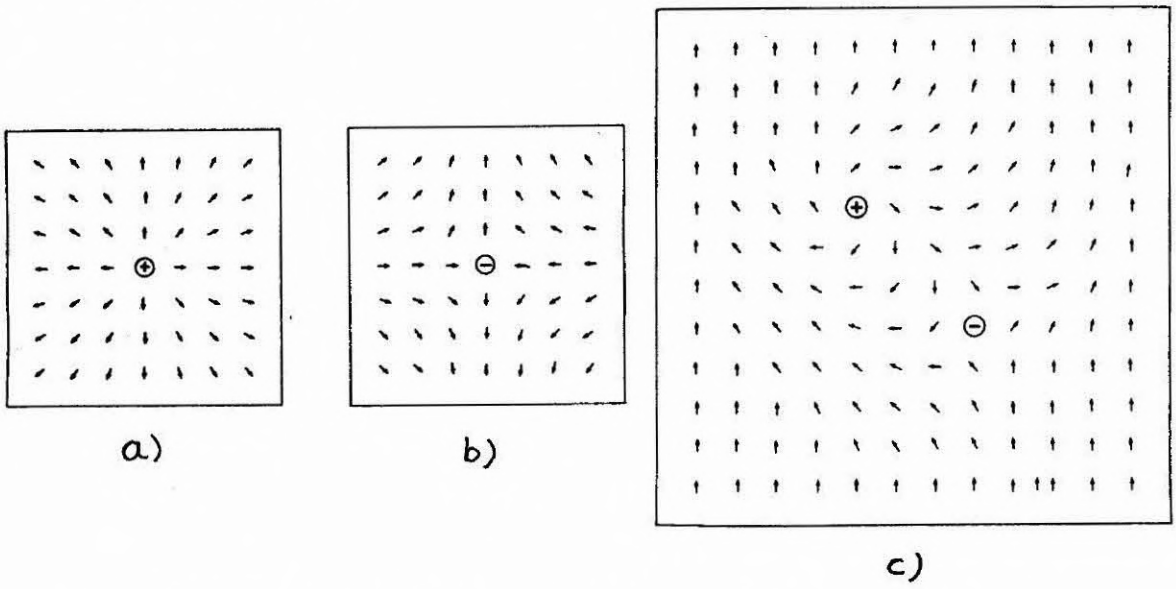

Figure 2.2 Vortex and antivortex excitations. a) vortex; b) antivortex and c) vortex-antivortex pair.

The energy of such a vortex is

$$E \simeq \pi J \ln \frac{L}{a_o} \tag{2.17}$$

where L is the dimension of the system and a_o is a lower cutoff. So a single vortex costs an infinite amount of energy. However a vortex pair of opposite vorticities (Figure 2.2) has a

finite energy

$$E_{pair} = 2\pi J \ln(\frac{|\vec{r}_1 - \vec{r}_2|}{a_0}) \tag{2.18}$$

At low temperatures vortices are therefore bound in pairs. However at sufficiently high temperatures isolated vortices will appear due to the resulting gain in entropy. The entropy of a single vortex is

$$S = 2k_B \ln \frac{L}{a_o} \tag{2.19}$$

So the free energy is $F = (\pi J - 2k_B T) \ln \frac{L}{a_o}$ and it is zero at

$$k_B T_c = \frac{\pi J}{2} \tag{2.20}$$

This indicates that there is a finite temperature T_c above which isolated vortices are favorable. Although the system does not have an ordered phase below T_c, topological order exists. The topological order is lost as soon as vortices are energetically favorable.

In order to obtain a tractable theory, Kosterlitz and Thouless assume spin-wave excitations superimposed on vortex configurations. The neglect of spin-wave vortex interactions can be shown to be exact in the Villain's approximation (see Appendix C). The Hamiltonian thus breaks up into independent spin-wave and vortex parts. The vortex part of the Hamiltonian gives

$$-\frac{H}{k_B T} = \pi K \sum_{R,R'} M_R M_{R'} \ln \frac{|\vec{R} - \vec{R'}|}{a_o} + lny \sum_R M_R^2 \tag{2.21}$$

where $M_R = \pm 1$ is the winding number of a vortex with center at $\vec{R}$, $K = J/k_B T$ and $y = e^{-E_c/k_B T}$ where E_c is a core energy. The vorticities satisfy the neutrality condition

$$\sum_R M_R = 0 \tag{2.22}$$

Expression (2.21) corresponds to a coulomb gas Hamiltonian with charges $q = \sqrt{\pi K} M_R$. The number of charges is not conserved so y is the equivalent of the fugacity in a grand-canonical ensemble.

Renormalization-group methods were first used by Kosterlitz (1974) and applied directly to the Coulomb gas representation (2.21). Later, several authors have also obtained the same end result via other methods (see for example José et al, 1977; Young, 1978; Kogut, 1979). In Appendix C we discuss the derivation of renormalization-group equations for a more general problem involving different kinds of charges. The recursion relations for the Hamiltonian (2.21) are given by

$$\begin{aligned} \frac{dK^{-1}(l)}{dl} &= 4\pi^3 y^2(l) \\ \frac{dy(l)}{dl} &= (2 - \pi K(l))y(l) \end{aligned} \tag{2.23}$$

where distances are scaled by a factor of e^l.

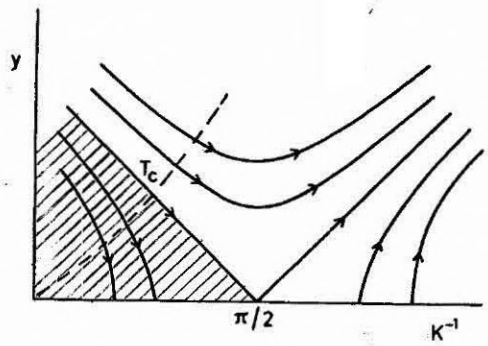

Figure 2.3 Renormalization-group trajectories. The shaded region is a domain of attraction of the line $y(l) = 0$. Dotted line represents a locus of initial conditions.

The analysis of these recursion relations provides the behavior of $K(\infty)$, the renormalized value of the coupling, and the critical exponents. The Hamiltonian trajectories generated by (2.23) in the (K^{-1}, y) plane are shown in Figure 2.3, together with the locus of initial conditions $y = e^{-E_c/k_B T}$. Hamiltonians to the left of the incoming separatrix renormalize into a line of fixed points at $y = 0$, which describes the low temperature phase

where vortices are irrelevant. At higher temperatures, $y(l)$ eventually becomes large, indicating that vortices are important even at long wavelengths. In this phase the correlation function decays exponentially as

$$< e^{i(\theta_r - \theta_o)} >= e^{-r/\xi_+} \tag{2.24}$$

where the correlation length ξ_+ is related to the density of free vortices by

$$n_f(T) \simeq \xi_+^{-2}(T) \tag{2.25}$$

The renormalized value of K approaches the universal value $2/\pi$ as

$$K(\infty) = \frac{2}{\pi} + C|t|^{\nu}, \qquad T \rightarrow T_c^- \tag{2.26}$$

where $t = \frac{T - T_c}{T_c}$ is the reduced temperature and $\nu = 1/2$. The behavior of the correlation length above T_c can be evaluated from the recursion relations and turns out to be

$$\xi_+(T) \simeq e^{\frac{b'}{|t|^{\nu}}} \tag{2.27}$$

where b' is a non-universal constant.

The critical temperature itself is found by the intersection of the initial conditions (dotted line in Figure 2.3) and the separatrix of the renormalization-group flows. To first order in the fugacity, it is found to be

$$\frac{\pi J}{k_B T_c} - 1 = 2\pi e^{-E_c/k_B T} \tag{2.28}$$

2.3.2 Resistive behavior of the array

Using the current-phase relationship for a superconductor with uniform order parameter

$$j_S = \frac{n_s \hbar e}{m}(\vec{\nabla}\theta - \frac{2e}{\hbar c}\vec{A}) \tag{2.29}$$

where $n_s = |\Psi|^2$, we see ($A = 0$ in the present case) that a vortex on the phases of the XY model (2.3) corresponds to a vortex of supercurrent in the superconductor array with tangential component

$$j_S = \frac{n_S \hbar e}{m} \frac{1}{r} \hat{\theta} \tag{2.30}$$

The resistive behavior of the array is connected with the presence of free vortices. A current flowing through the superconductor in the presence of free vortices, creates a dissipative mechanism which cause a resistive behavior. The origin of this dissipation is the Lorentz force acting on a vortex when a current flows (see for example Tinkham, 1975)

$$\vec{F} = \vec{J} \times \vec{\Phi}/c \tag{2.31}$$

where Φ is the magnetic flux enclosed by the vortex. This arises because of the induced magnetic field due to the vortex current so the force is basically given by $\vec{F} = \frac{\vec{J}}{c} \times \vec{B}$. Due to this force vortices tend to move transverse to the flowing current. Suppose they move with drift velocity v, then they induce an electric field of magnitude

$$\vec{E} = \vec{B} \times \frac{\vec{v}}{c} \tag{2.32}$$

which is paralell to $\vec{J}$. This act like a resistive voltage and power is dissipated.

When a net flux of vortices exists, a voltage drop is developed between the ends of the superconductor. This voltage drop can be obtained by using the Josephson relation

$$\Delta V = \frac{\hbar}{2e} \frac{d}{dt} \Delta\theta \tag{2.33}$$

where ΔV is the voltage drop. $\Delta\theta$ is the phase difference between the ends of the sample. So if a phase difference proportional to t exists a constant voltage drop will be generated. Now a phase slip of 2π occurs whenever a vortex crosses the width of the sample. This can be understood by Figure 2.4. Consider points A and B at the ends of the sample. If a vortex is all the way to the right, the phase difference $\theta_A - \theta_B = 0$ and it goes to $\theta_A - \theta_B = 2\pi$ when the vortex is finally at the left side.

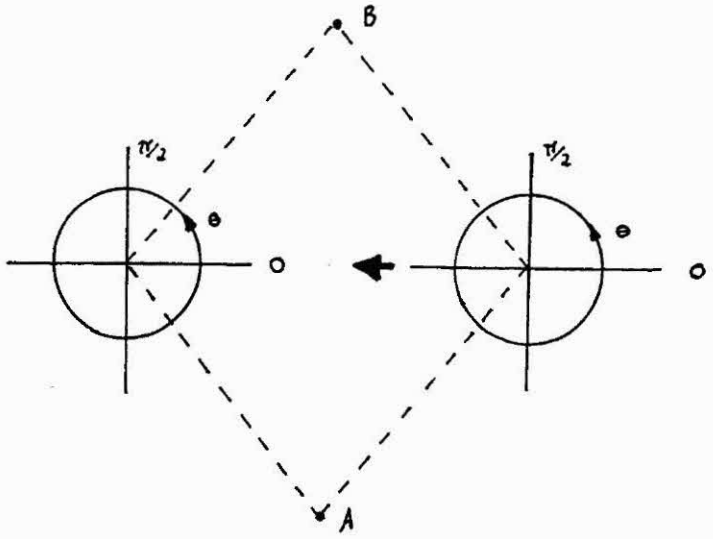

Figure 2.4 Phase slip due to a vortex. When a vortex cross the width of the sample from right to left it causes a change of phase of 2π between points A and B at the ends of the sample.

Now if we have n_f free vortices with drift velocity v_D then

$$\frac{d\Delta\theta}{dt} = 2\pi L n_f |v_D| \tag{2.34}$$

where L is the length of the system. $|v_D|$ comes from the different directions of the vortices of opposite signs. Since the drift velocity is proportional to the Lorentz force due to the viscous damping (neglect pinning) we have

$$v_D = \mu F \propto \mu I \tag{2.35}$$

Combining these equations, we obtain

$$\frac{d\Delta\theta}{dt} \propto L n_f \mu I \tag{2.36}$$

and the resistance per square is therefore given by

$$R \propto \mu n_f \tag{2.37}$$

i.e., it is proportional to the mobility and density of free vortices.

Using this result together with (2.25) and (2.27) we get

$$R = a\mu e^{-b_2 \frac{1}{t^{1/2}}} \tag{2.38}$$

Thus we expect that at $H = 0$ and above T_c the resistance has a exponential behavior. Below T_c since vortices are bound in neutral pairs, there is no phase slip process and $R = 0$. Actually, below T_c, R is not exactly zero due to finite current and finite size effects (Nelson and Halperin, 1978). Figure 2.5 summarizes the behavior described in this Section.

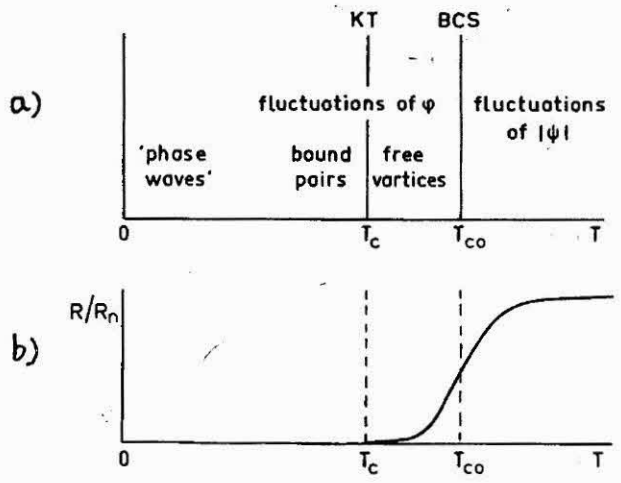

Figure 2.5 Resistive behavior of the array. a) Schematic diagram of the successive transitions; b) Schematic behavior of the resistance as a function of temperature for a two-dimensional superconducting array.

2.4 Finite-field effects

In the presence of an external field the vortex unibinding mechanism described in Section 2.3 is certainly more complicated.

If we consider a continuous version of the array problem, i.e., a two-dimensional superconducting film, magnetic flux can only penetrate in form of quantized vortices. As described in Section 2.3, under the influence of the Lorentz force from a driving current, the vortex motion gives rise to a non-zero resistance. At zero external field, vortices can

only appear as a result of thermal excitation. At low temperatures and zero magnetic field, vortices can appear only in bound pairs with total vorticity zero and so the resistance of the array is zero. A magnetic field induces vortices of one polarity in addition to any thermally excited ones. In the absence of thermal excitations or substrate potential, the mutual repulsion of the vortices would lead to a regular triangular lattice, with spacing determined only by the external magnetic field. It is not clear if this picture can also be applied to the arrays that have been studied experimentally, but one can already realize that this natural periodicity imposed by the external field will compete with the period of the underlying substrate potential of the array. Thus it is natural to suggest that this may lead to commensurate-incommensurate transitions effects when the external field is varied.

2.4.1 Mean-field theory results

Mean field theory provides a rough way to approach this problem for general f. Mean field theory however is well known to be inadequate to understanding two-dimensional systems and may even lead to misleading results. The application of this approximation to the superconducting arrays has been pursued by Rammal et al (1983) and Shih and Stroud (1983). Figure 2.6 shows the mean-field transition temperatures for the triangular and honeycomb lattices. They are not very illuminating. The most striking feature however is their irregularity.

If the mean-field equations are linearized about the transition tenperatures, it is found (Shih and Stroud, 1985)

$$\eta_r - \frac{1}{2k_B T} \sum_{r'} J e^{iA_{rr'}} \eta_{r'} = 0 \tag{2.39}$$

where $\eta_r =< e^{i\theta_r} >$ is the mean-field order parameter. Equation (2.39) is precisely the Shroedinger equation in the tight-binding representation for an "electron" of charge $2e$ in a magnetic field B and moving in a lattice. The order parameter η_r is the analog of the complex wave function at site $\vec{r}$, J is the hopping integral and $\beta = \frac{1}{k_B T}$ is the energy eigenvalues. T_c is the highest value of T for which the mean field equations have a non-trivial

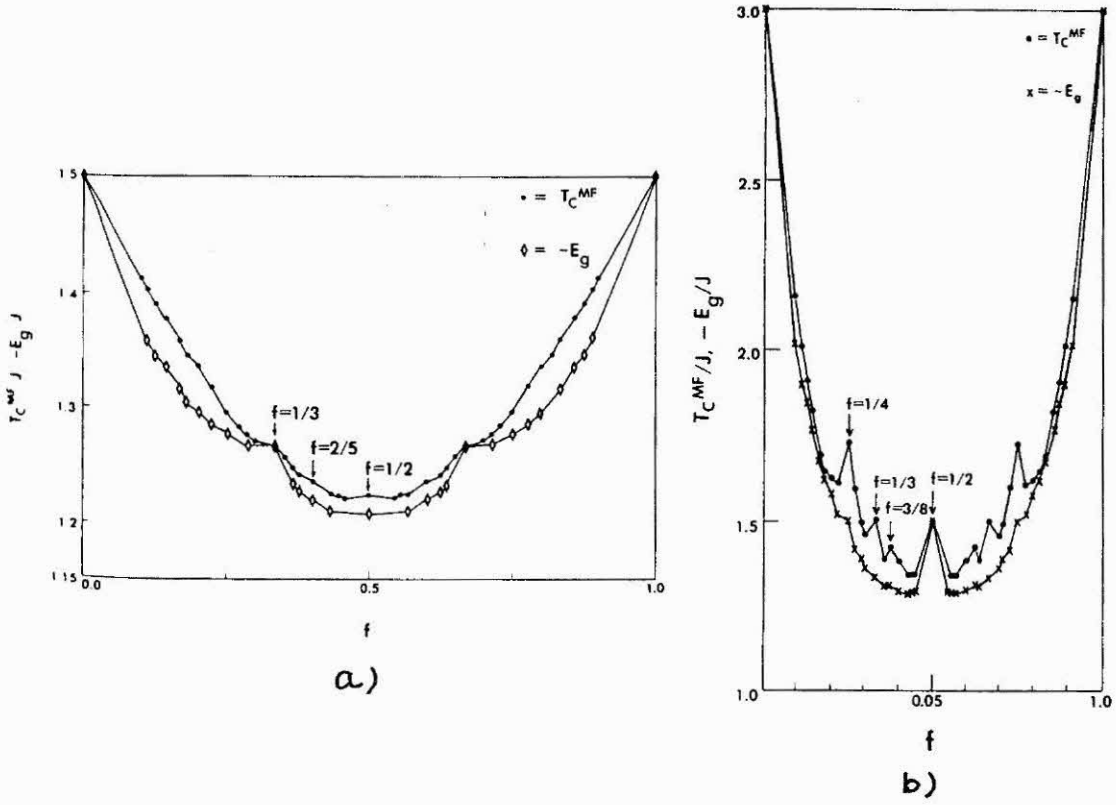

Figure 2.6 Mean-field transition temperatures and ground-state energies. a) honeycomb and b) triangular lattice (Shih and Stroud, 1985).

solution, i.e., it maps directly onto the band edge of the tight-binding electron problem. These band edges have been worked out by Hofstadter (1976) for the square lattice and by Claro and Wannier (1979) for a triangular lattice.

Figure 2.6 also shows certain characteristic differences between the lattices. The triangular lattice for example, as well as the square lattice, shows a secondary minimum at $f = 1/2$ which is very weak or non-existent for the honeycomb lattice. Evidence of this lattice dependence has been seen experimentally (Resnick et al, 1984).

2.4.2 Coulomb-gas representation

Familiarity with the coulomb gas representation for the XY model discussed in Section 2.3 would suggest that much insight into the problem can be obtained by isolating from (2.5) the vortex interaction terms. This can be acomplished by a very systematic procedure for handling problems like this, introduced by José et al (1977).

To preserve the periodicity of the cosine term in (2.5), first expand into a Fourier series

as

$$e^{K\cos(\theta_r - \theta_{r'} - A_{rr'})} = \sum_{s_{rr'}=-\infty}^{\infty} I_{s_{rr'}}(K) e^{is_{rr'}(\theta_r - \theta_{r'} - A_{rr'})} \tag{2.40}$$

The Fourier components are just Bessel functions of order $s_{rr'}$. In the limit of large coupling this reduces to

$$I_{s_{rr'}}(K) \simeq \frac{e^K}{(2\pi K)^{\frac{1}{2}}} e^{-\frac{{s_{rr'}}^2}{2K}} \tag{2.41}$$

When (2.40) is substituted in the partition function (2.9), the integrations in the θ variables induce the constraint

$$\prod_r \delta_{\sum_{r'} s_{rr'},0} \tag{2.42}$$

were $\sum_{rr'}$ is a sum over all nearest neighbors $\vec{r'}$ and $s_{rr'} = -s_{r'r}$. This constraint can be automatically satisfied if we define new integer variables on the sites $\vec{R}$ of the dual lattice,i.e., the lattice formed by the centers of the plaquettes, by

$$\sum_R s_{rr'} = M_R \tag{2.43}$$

where $\sum_R$ indicates a directed sum over the bonds surrounding the plaquette with dual site $\vec{R}$. Using the constraint (2.43), the partition function in terms of these new variables is

$$Z = \left[\prod_R \sum_{M_R}\right] e^{-\frac{1}{2K}\sum_{<RR'>}(M_R - M_{R'})^2 - 2\pi f i \sum_R M_R} \tag{2.44}$$

When $f = 0$ the above expression is the partition function of the discrete gaussian model of Chui and Weeks (1976) used in the study of crystal growth. If $f \neq 0$ the discrete gaussian model is subject to an imaginary field. The above expression can also be viewed as a correlation function of the discrete gaussian model (with $f = 0$) (Fradkin et al, 1979).

One would like to replace the integer valued field M_R by an ordinary scalar field ϕ. The necessary manipulation is provided by the Poisson summation formula

$$\sum_{m=-\infty}^{\infty} g(m) = \sum_{m=-\infty}^{\infty} \int_{-\infty}^{\infty} d\phi\, g(\phi) e^{-2\pi m\phi i} \tag{2.45}$$

where g is an arbitrary function.

Applying this identity to (2.44) and performing the resulting gaussian integral gives

$$Z = Z_{sw} \left[\prod_R \sum_{M_R} \right] e^{-\pi K \sum_{R,R'} (M_R - f) G(R - R') (M_{R'} - f)} \tag{2.46}$$

where Z_{sw} results from the gaussian integration and can be identified as the spin wave contribution whereas M_R can be identified as the vortex winding number. The large distance behavior of $G(R - R')$ is given by (Appendix B)

$$G(R - R') = \ln \frac{|R - R'|}{a} + \frac{\pi}{2} \tag{2.47}$$

and the M_R satisfy the neutrality condition

$$\sum_R M_R = 0 \tag{2.48}$$

So the model (2.5) has been mapped into a coulomb gas of integer charges M_R interacting with a background of frozen in fractional charges f. For $f = 0$ we recover the XY model. As mentioned before in this approximation spin waves and vortices decouple. Since the spin waves alone do not drive the phase transition, we need only to consider the coulomb gas contribution.

2.4.3 Ground states for rational f.

In the ground state the lowest possible M_R consists of $M_R = 0$ and $M_R = 1$, arranged in such a way that $\sum_R (M_R - f) = 0$. Therefore we need f vortices of charge $M_R = 1$ and $(1 - f)$ vortices of charge $M_R = 0$.

Teitel and Jayaprakash (1983a) have performed computer simulations in the charge model (2.46) for rational values of $f = p/q$, assuming the ground state has periodicity $q \times q$. For several f, the $q \times q$ assumption was checked by calculating on $nq \times nq$ lattices. Figure 2.7 shows the results of this calculation.

Figure 2.8 also shows the calculated critical current of the array as a function of f, using Monte Carlo simulations. Note the large variations of $i_c(f)$ as a function of f. Working out

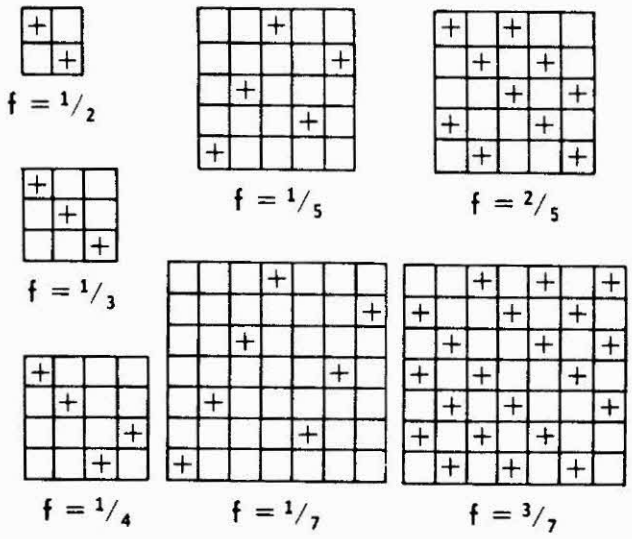

Figure 2.7 Ground state configurations in the charge model. A plus denotes a charge $1-f$, i.e., a vortex in the phase θ, while an empty box denotes a charge $-f$ (Teitel and Jayaprakash, 1983a).

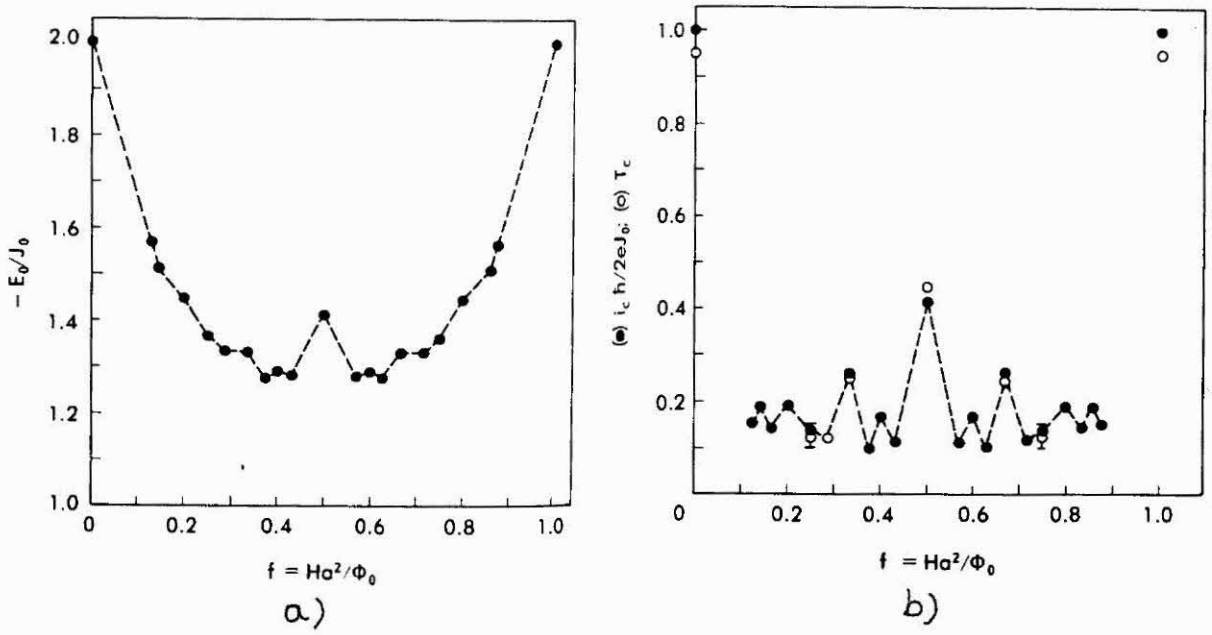

Figure 2.8 Critical temperatures and ground state energies. a) Ground state energies for several rational f; b) Zero-temperature critical currents (solid circles) and zero-current critical temperatures T_c (open circles) (Teitel and Jayaprakash, 1983a).

the mathematical expression for i_c, they were also able to establish a bound for the value

of the critical current

$$i_c(p/q) \leq \frac{\pi}{q}\left|\frac{e}{\hbar}E_o(f)\right| \tag{2.49}$$

where $E_o(f)$ is the ground state energy. So $i_c(f)$ exhibits a dramatic discontinuity variation as a function of f. From energetic grounds and at $i = 0$ but finite T one would expect

$$k_B T_c(f) \leq \left(\frac{\hbar}{2e}\right) i_c(f) \tag{2.50}$$

since when T is large enough to produce an average current fluctuation in the array of order i_c, vortices of current will appear an be able to move, and a resistive transition will occur.

Noting that the values calculated by Monte Carlo simulation satisfy this relation, equation (2.49) and (2.50) can be combined to give a bound on $T_c(f)$ as

$$k_B T_c(p/q) \leq \frac{\pi}{2q}\left|E_o(f)\right| \tag{2.51}$$

Note the dependence in q, it is crucial. For irrational f, $q \to \infty$ and $T_c(f) = 0$. Let us now consider the implications of these relations for the array resistance $R(T,f)$. Consider a given $f_o = p_o/q_o$, for p/q sufficiently close to f_o, all rational numbers satisfy $q \gg q_o$ and so using (2.51) $T_c(f) < T(f_o)$. Now consider a temperature T such that $T(f) < T < T(f_o)$. Then $R(T,f_o) = 0$ and $R(T,f) > 0$. Since for $f \simeq f_o$ we can regard the ground state of f as that of f_o with a superlattice of defects or domain walls to ensure charge neutrality (see Figure 2.9), the number of these defects is proportional to $|f - f_o|$, then around $f \simeq f_o$ we can assume they density is $\propto |f - f_o|$.

Now for $T < T_c(f)$ these defects can not move since they are pinned and therefore $R(f) \to 0$, so we can assume that for $T > T_c(f)$ they unpin and this motion like the free vortex motion causes the nonzero R. Since resistance is proportional to number of free defects we find for $f \simeq f_o$ that

$$R(T,f) \propto |f - f_o| \tag{2.52}$$

So a cusp in the resistance curve is predicted. A plot of $R \times H$ is sketched in Figure 2.10. Note that as T is lowered more and more structure appears besides the dip at $f = 1/2$.

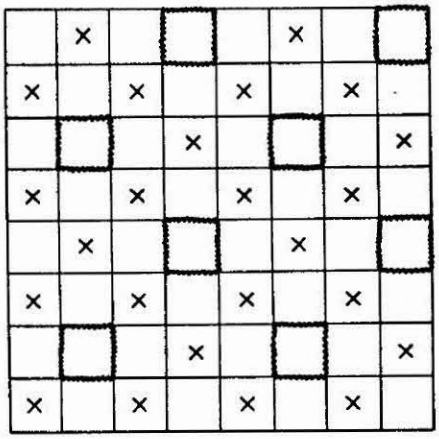

Figure 2.9 A ground state with defects. Ground state for $f = 3/8$ constructed from the ground state of $f = 1/2$ with a superlattice of vacancies.

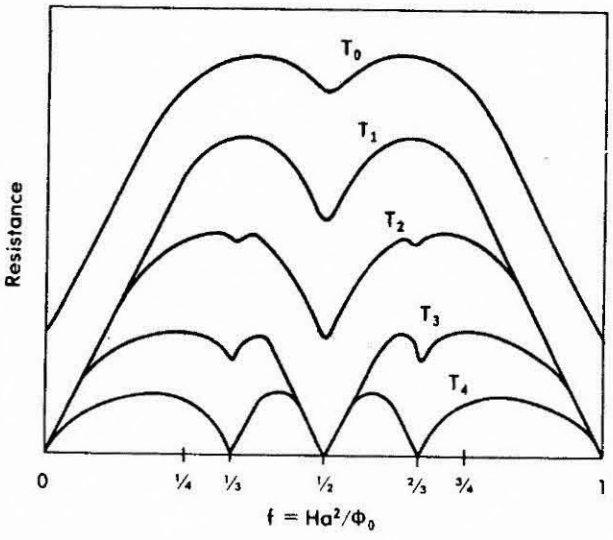

Figure 2.10 Resistance as a function of temperature. Schematic plot of resistance as a function of magnetic field for a sequence of temperatures $T_4 < T_c(1/3) < T_3 < T_c(1/2) < T_o < T_1$ (Teitel and Jayaprakash, 1983a).

These dips at other rational values have not clearly been observed in arrays although some evidence was observed in wire networks (Pannetier et al, 1983).

If we look at the ground states obtained by numerical simulations in the range $\frac{1}{3} \leq f \leq \frac{1}{2}$

it is apparent that they could be generated from the $f = 1/2$ ground state by introducing domain walls (see Figure 2.11 for an example). Note that this structure of domains is a quasi-onedimensional structure. Halsey (1985a) has pursued this matter further and with the assumption of one-dimensionality he found exact results for the ground state energy.

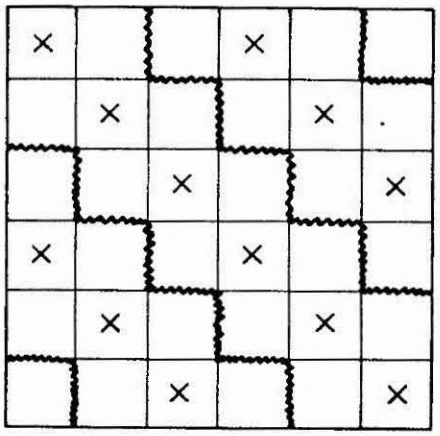

Figure 2.11 Ground state of $f = 1/3$. This ground state can be constructed from the $1/2$ case by introducing a structure of domain walls.

2.4.4 Landau-Ginzburg-Wilson free energy.

A useful approach to study the system at higher temperatures and the universality class of the transitions at various values of f is to construct Landau-Ginzburg-Wilson (LGW) free energies. Choi and Doniach (1985) have constructed LGW free energies using a Hubbard-Stratonovich transformation (Hubbard, 1959; Stratonovich, 1957) for simple values of f and for triangular and square lattices.

First rewrite equation (2.5) in the form

$$-\frac{H}{k_B T} = \frac{1}{2}\sum_{rr'} u_r^* P_{rr'} u_{r'} - K_N \tag{2.53}$$

where

$$P_{rr'} = K_{rr'} e^{-iA_{rr'}} + \delta_{rr'} \sum_{rr'} K_{rr'} \tag{2.54}$$

and $u_r = e^{i\theta_r}$. Here $K_{rr'} = K$ for nearest neighbors and 0 otherwise. The second term in (2.54) has been introduced to make the $P_{rr'}$ positive definite. The Hubbard-Stratonovich transform makes use of the gaussian identity

$$\left[\prod_r \int dz_r \int dz_r^*\right] e^{-\frac{1}{2} z_r^* P_{rr'}^{-1} z_{r'} + \frac{1}{2}(u_r^* z_r + u_r z_r^*)} = \sqrt{2\pi\, det P_{rr'}}\, e^{\frac{1}{2} u_r^* P_{rr'} u_{r'}} \tag{2.55}$$

Applying this transformation to (2.9) we obtain, omiting overall constants

$$Z = \left[\prod_r \int dz_r \int dz_r^*\right] e^{-\frac{1}{2} z_r^* P_{rr'}^{-1} z_{r'} + \sum_r \ln I_o(|z_r|)} \tag{2.56}$$

where I_o is the Bessel function. The standard procedure now is to expand the Bessel function and keep only the relevant terms

$$I_o(x) = \frac{1}{4}x^2 - \frac{1}{64}x^4 \ldots \tag{2.57}$$

Note that due to the form of the matrix $P_{rr'}$ in (2.54), the exponent is not diagonalized by a simple Fourier transform. However a LGW free energy can be obtained directly by diagonalizing the resulting Fourier transformed matrix $P_{qq'}$ and expanding about the modes corresponding to the maximum eigenvalues of this matrix. For example, for $f = 1/2$ on a square lattice it is found (Choi and Doniach, 1985)

$$Z = \left[\prod_r \int d\Psi_r \int d\Phi_r\right] e^{-F(\Psi,\Phi)} \tag{2.58}$$

where

$$\begin{aligned} F(\Psi,\Phi) = \int\int dxdy \Big[& \frac{r}{2}(|\Psi|^2 + |\Phi|^2) + \frac{e}{2}(|\nabla\Psi|^2 + |\nabla\Phi|^2) \\ & + \frac{u}{4}(|\Psi|^2 + |\Phi|^2)^2 + v|\Psi|^2|\Phi|^2 \\ & + u'|\Psi|^2|\Phi|^2 \cos 2(\theta - \phi)\Big] \end{aligned} \tag{2.59}$$

and $r = (\frac{1}{\lambda(Q_{1,2})} - \frac{1}{2})$. $e, u > 0$ and $v < 0$ are constants which can be calculated directly from the matrices that diagonalize $P_{q,q'}$. Here $\Psi = |\Psi| e^{i\theta}$ and $\Phi = |\Phi| e^{i\phi}$ measure fluctuations about the modes Q_1 and Q_2 corresponding to the two degenerate maxima of $P_{q,q'}$.

However, some care should be taken with this procedure because it can lead to misleading results. For $f = 1/4$, for example, on a triangular lattice, Choi and Doniach found the

same expression as (2.59). This could imply that these two different cases have the same critical behavior. The numerical results of Shih and Stroud (1985), however, shows that this is not the case.

For $f = 1/2$ on a triangular lattice they found an expression similar to (2.59), but the coupling between the phases now occuring in the sixth order term of the expansion which gives $\cos 3(\theta - \phi)$ instead of the last term appearing in (2.59). This is in disagreement with Yosefin and Domany (1985) who derived LGW free energies using symmetry arguments. These authors obtained similar expressions as (2.59) for square and triangular lattices but with $u' > 0$. The sign of u' is crucial here. In two dimensions one assumes that the phase transiton occurs well below the mean-field critical temeprature due to fluctuations. Amplitudes fluctuations in Ψ and Φ are irrelevant near two dimensions (see for example, Nelson, 1983), so $|\Psi|^2$ and $|\Phi|^2$ are well approximated by their mean-field values. If we minimize (2.59) we find that if $u' > 0$ either $|\Psi| = 0$ or $|\Phi| = 0$. In this case Yosefin and Domany have shown that higher other terms are irrelevant. On the other hand, if $u' < 0$ then the minimum of the free energy occurs for $\Psi = \Phi$ with

$$|\Psi|^2 = -\frac{r}{2(u + v - u')} \tag{2.60}$$

In this case, a lattice version of (2.59) can be written as

$$A = \alpha \sum_{<rr'>} [cos(\theta_r - \theta_{r'}) + cos(\phi_r - \phi_{r'})] + h \sum_r cos2(\theta_r - \phi_r) \tag{2.61}$$

where α is proportional to $|\Psi|^2$ given by (2.60). When $u' > 0$, one arrive at the same result after performing a change of variables $\Psi - \Phi \rightarrow \Psi$ and $\Psi + \Phi \rightarrow \Phi$.

2.5 The fully frustrated XY model

Of course, the detailed nature of the phase transitons at the several non-integer values of f is a complicated problem. However, one would expect to be able to understand the behavior for simple values of f. In particular, the fully frustrated case, i.e., $f = 1/2$ is a

very interesting one because it is connected with different problems (Villain, 1977; Halsey, 1985b).

Teitel and Jayaprakash (1983b) have performed numerical simulations for the $f = 1/2$ case on a square lattice. Results for the helicity modulus and specific heat are shown in Figures 2.12 and 2.13 respectively.

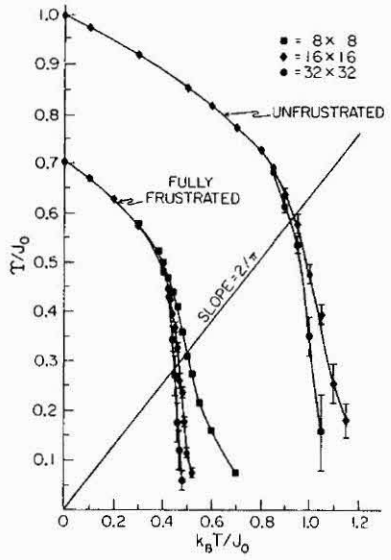

Figure 2.12 Helicity modulus for $f = 1/2$. Helicity modulus $Y(T)$ as a function of temperature of the unfrustrated case ($f = 0$) and fully frustrated case ($f = 1/2$) on a square lattice. The line of slope $2/\pi$ indicates the universal jump predicition for the KT transition (Teitel and Jayaprakash, 1983b).

The helicity modulus $Y(T)$ measures the stiffness of the system when a long-wavelength twist is applied to the phases. It is directly related to the renormalized value of the coupling constant K_R in the unfrustrated case. In this case due to the behavior of K_R as the transition is aproached from below described by equation (2.26), a universal jump of this quantity has been predicted by Nelson and Kosterlitz (1977). In terms of the helicity modulus one expects

$$\lim_{T \to T_c^-} Y(T)/k_B T = \frac{2}{\pi} \tag{2.62}$$

The line of slope $2/\pi$ in Figure 2.12, indicates the universal jump prediction for the

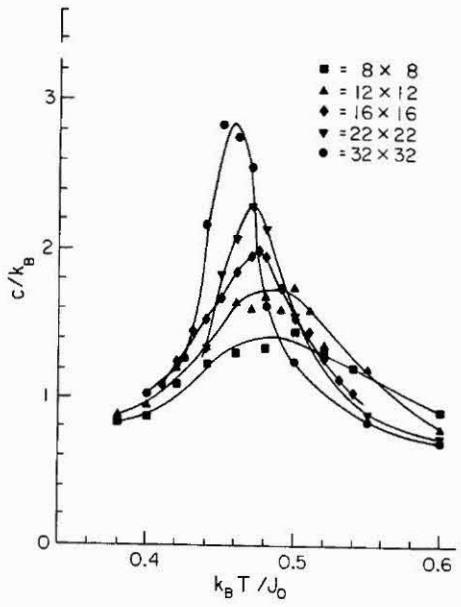

Figure 2.13 Specific heat for $f = 1/2$.(Teitel and Jayaprakash, 1983b).

Kosterlitz-Thouless transition. Finite size effects have broadened the discontinous jump but from its position the transition temperature for the unfrustrated case is estimated to be $kT_c \simeq 0.95J$. For the fully frustrated case Figure 2.12 shows a clear evidence for a phase transition at a finite temperature $k_B\, T_c \simeq 0.45J$ but it goes more steeply than in the unfrustrated case and is inconsistent with the universal jump prediction, having a jump larger that the Nelson-Kosterlitz result.

In marked contrast with the unfrustrated case in which the peak of the specific heat saturates at a finite value about $1.5k_B$, the specific heat peak diverges linearly with the size of the system in the frustrated case. This implies a logarithmic singularity as in the Ising model. It also occurs roughly at the same temperature in which $Y \rightarrow 0$. Similar results have been found by Shih and Stroud (1985) for the triangular lattice. For the honeycomb lattice however no specific heat divergence is observed. Instead for this case the ground state configuration is multiply degenerate.

To understand the numerical results we have to look at the excitations above the ground state and study the mechanism by which a phase transition could occur.

The doubly degenerate ground state of the fully frustrated XY model on a square lattice

(Figure 2.1) has a bond phase difference of $\pm\pi/4$ and a ground state energy of $\sqrt{2}J$ per site. We recall that in the coulomb gas representation the ground state has a chessboard structure consisting of charges $q = \frac{\sqrt{2\pi}}{2} J$ (Figure 2.14). In this representation the ground state is clearly doubly degenerate since one can replace $q \rightarrow -q$ leaving the total energy unchanged. If we identify the + and − charges as "up" and "down" spins, respectively, the model maps into a long-range Ising antiferromagnet with conserved magnetization. Unfortunately one can not do too much with this. There are two types of excitations in the ground state: domain walls and vortex pairs. A vortex pair result from interchanging + and − in a given pair with separation r and must have an energy proportional to $\ln r$. Domain walls are Ising type excitations and come from the double degeneracy of the ground state.

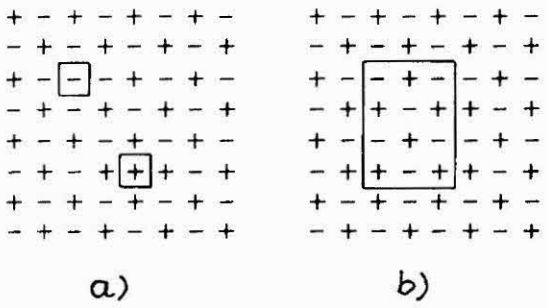

Figure 2.14 Ground state excitations. Two types of excitations for the $f = 1/2$. a) vortex pair; b) closed domain wall.

Consider small phase deviations above the ground state, then from (2.5) we obtain

$$H = -\frac{J}{\sqrt{2}} \sum_{<rr'>} \cos(\theta_r - \theta_{r'}) \tag{2.63}$$

which gives an XY-like transition about

$$k_B T_v = \frac{\pi J}{2\sqrt{2}}$$

For an infinite straight domain wall, the excitation energy can be calculated in a straightforward way in the coulomb gas representation (Appendix A). Halsey (1985b) has obtained numericaly similar results in the phase model. We obtain

$$E_W = 0.27J \tag{2.64}$$

It also follows from the same calculation that the interaction between two parallel infinite domain walls separated by a distance $\vec{R}$ is given by

$$E_{int} = 2q^2 e^{-\pi \frac{R}{a}} \tag{2.65}$$

If we disregard the effects of the corners of a closed domain wall, the energy of the domain should be proportional to the perimeter. Using a Peierls energy-entropy argument to estimate the temperature in which the free energy of a closed domain is zero, one finds

$$k_B T_s = E_w / \ln 3 \tag{2.66}$$

Since $T_s < T_v$, this suggests that two phase transitions can occur with increasing temperature, leaving an intermediate phase with Ising-like disorder and XY-like order. However, as pointed out by Halsey (1985b), the corners of a close domain wall behave as fractional charges. If we define an average charge in each vertice by the average of four neighboring plaquettes, the sides of the domain average to zero, but the corner average to $\frac{1}{4}q$. From the geometry of a domain we can see that if the domain is neutral, the sum of the corner charges is zero otherwise it is not zero. A simple estimate of the critical temperature for the unbinding of corner charges in a neutral large domain gives $T_{\frac{1}{4}v} \simeq \frac{1}{16} T_v$. Comparing the estimates we have $T_{\frac{1}{4}v} < T_s < T_v$. Thus when the free energy of a domain wall goes to zero free corner charges are available which presumably unbind immediatly the integer vortices. The important point here is that the Ising transition will correspond not merely to a proliferation of domain walls but to a proliferation of domain walls carrying free corner charges, and these may cause a direct transition to a disordered XY-like phase.

One can already see that in order to study the phase transition in more detail one then needs an effective Hamiltonian which contains vortices and domain walls explicitly. The two coupled XY models obtained in (2.58) provides a convenient representation to carry out such an analysis.

Chapter 3

CRITICAL BEHAVIOR OF COUPLED XY MODELS

3.1 Introduction

In this section we analyse the critical behavior of an array with a half flux quantum per plaquette. As discussed in Section 2.5, in a triangular or square lattice, this corresponds to a class of XY models where the ground state exhibit both continuous and discrete degeneracy simultaneously. Other models such as the antiferromagnetic XY model on a triangular lattice (Lee et al, 1986), the double-layer XY model (Parga and Himbergen, 1980) and the helical XY model (Garel and Doniach, 1980) are also included.

As shown in Section 2.4, the LGW free energy for the fully frustrated case leads to a coupled XY problem. The other models mentioned above can also be described by the same free energy. We therefore consider a coupled XY model described by the action

$$A = -\frac{H}{k_B T} = \alpha \sum_{<rr'>} \cos(\theta_r - \theta_{r'}) + \beta \sum_{<rr'>} \cos(\phi_r - \phi_{r'}) + h \sum_r \cos p(\theta_r - \phi_r) \qquad (3.1)$$

where p is an integer and θ_r, ϕ_r are phases defined at the sites $\vec{r}$ of a square lattice with lattice spacing a.

We study the phase transition in coupled XY models using renormalization-group arguments (Granato and Kosterlitz, 1986a). We analyse this model for $p = 2$ and $p = 3$ which seems to be the relevant cases with respect to the superconducting array problem. The model is transformed into an equivalent eletrodynamic representation and recursion relations for small vortex fugacities are derived. Migdal recursion relations are used to study the limit $h \to \infty$. A semi-qualitative analysis involving vortices and strings, using

a representation in which domain walls appear explicitly, is used to study the phase transitions. In particular, these arguments give some indication that the transition along the $\alpha = \beta$ line could be first order.

Figure 3.1 shows the resulting phase diagram. The line APB corresponds to an Ising ($p = 2$) or a 3-state Potts ($p = 3$) transition. If the initial points of the Hamiltonian are along the line $\alpha = \beta$ a single transition occurs separating a locked phase with XY and Ising ($p = 2$) order from a high-temperature XY and Ising disordered phase. The transition is a complicated point which can be denoted as tetracritical but in an as yet undetermined universality class. There are however some indications from the numerical work of Teitel and Jayaprakash (1983b), Lee et al (1986) and Berge et al (1986) that this point may have simultaneous Ising and XY-like behavior ($p = 2$). This problem has been studied by many authors with mixed success. It remains however an outstanding problem.

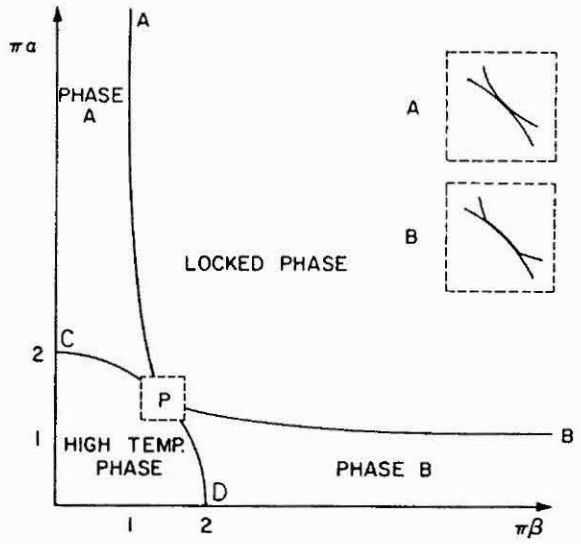

Figure 3.1 Topological features of the phase diagram. The manner the lines merge at P is not determined. Two possibilities are indicated in the insets A and B. Phases A and B are partial ordered phases.

The models mentioned before are represented by (3.1) with initial couplings $\alpha = \beta$. It can be shown that the $\alpha \neq \beta$ line represents a frustrated XY magnet on a square lattice in which the strength of the antiferromagnetic and ferromagnetic bonds are unequal

(Granato and Kosterlitz, 1986b). This latter model has been studied recently by Berge et al (1986) using Monte Carlo simulations. The frustration in each plaquette was made vary by changing the negative bond strength. From a ground state analysis they found that below a critical value of the ratio of 1/3 between the negative and positive bonds, the ground state is paramagnetic, while for ratios greater than 1/3 it is doubly degenerate with canted spin configurations. The phase diagram obtained by Monte Carlo simulations is shown in Figure 3.2. The low transition temperature corresponds to Ising type and the high transition temperature corresponds to the XY type when the bonds are of different strengths. In the fully frustrated case, when the bonds have the same strength, the two transitions merge into a single one of dominant Ising character.

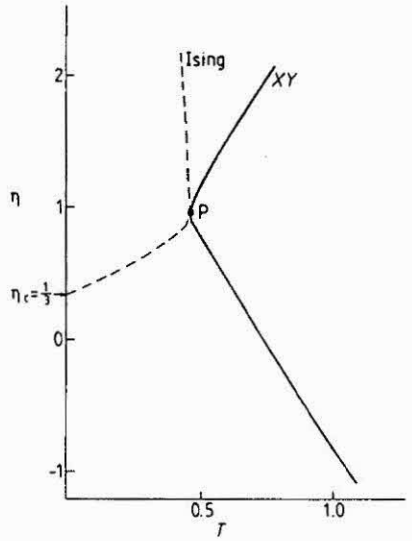

Figure 3.2 Phase diagram for the frustrated XY model. η is the ratio between the antiferromagnetic and ferromagnetic bonds. The nature of the phase transition at P is not determined (Berge et al, 1986).

Unfortunately our analyses cannot determine the behavior of the system on the $\alpha = \beta$ line except for arguments which are fairly conclusive that there is a single transition directly from a locked to disordered phase with no intervening phase with partial order as is the case for $p \geq 4$. Also, it cannot unambiguously determine whether the transition from the locked to disordered phase for $\alpha \approx \beta$ is a single transition or a double transition with an intervening

unlocked phase with algebraic order in one of the phase and disorder in the other. We incline to the view that there is such an unlocked phase in a region of the (α, β) plane except for a multicritical point on the $\alpha = \beta$ line. Thus we predict that such systems as the Josephson junction array on a square and triangular lattice with half a flux quantum per plaquette, the triangular XY antiferromagnet in zero magnetic field and the fully frustrated XY model on a square lattice, all have a single transition from the completely ordered to completely disordered phase.

Another model with similar properties is an XY model with interactions of different but commensurate periodicities

$$A = \alpha \sum_{<rr'>} \cos(\theta_r - \theta_{r'}) + \beta \sum_{<rr'>} \cos p(\theta_r - \theta_{r'}) \tag{3.2}$$

where the second term has periodicity $\theta \rightarrow \theta + 2\pi/p$. This model can be shown to be described by a similar model to that discussed in (3.1), with a slight modification in the coupling term

$$A = \alpha \sum_{<rr'>} \cos(\theta_r - \theta_{r'}) + \beta \sum_{<rr'>} \cos(\phi_r - \phi_{r'}) + h \sum_r \cos(p\theta_r - \phi_r) \tag{3.3}$$

The model defined by (3.2) has also been studied recently by Lee and Grinstein (1985) using a different analysis. In contrast to the fully frustrated case this model is not double degenerate. For $\alpha < 4\beta$ each bond however has a metastable minimum at $\theta_r - \theta_{r'} = \pi$ in addition to the absolute minimum at $\theta_r - \theta_{r'} = 0$. In addition to vortex excitations, the ground state also have excitations which consist of one-dimensional strings of antiparallel spins that terminate in half-integer vortices and antivortices (Figure 3.3). The phase diagram shown in Figure 3.4 consists of three phase separated by lines of conventional XY transitions and lines of Ising transitions. This model also has an interesting phase diagram when $\beta < 0$. However the action (3.3) is not appropriate to describe the behavior in this region of the phase diagram.

This model is not realized by a superconducting array, but it can be related to fluid layers of liquid crystal where the molecules make a constant angle θ, ϕ relative to the normal

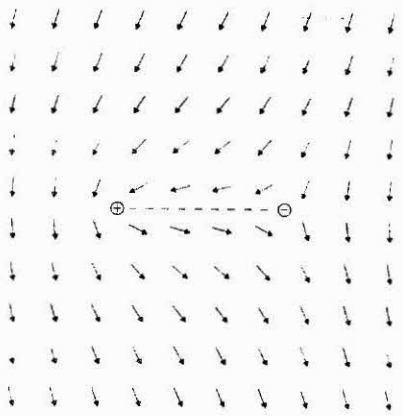

Figure 3.3 A half-integer vortex-antivortex pair connected by a string. The center of the half-integer vortices are represented by the circles with the plus and minus sign, and the string is represented by a dotted line (Lee and Grinstein, 1985).

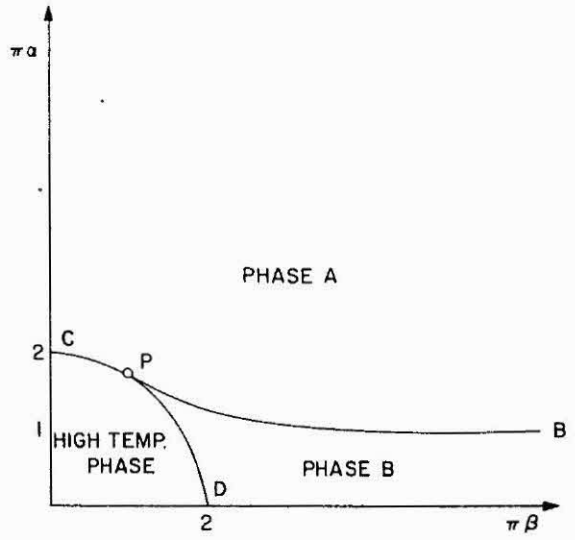

Figure 3.4 Schematic phase diagram for an XY model with competing periodicities. Phase A is a locked phase and phase B is a partial ordered unlocked phase.

to the plane. Then the local director is given by $n_r = (sin\phi cos\theta_r, sin\phi sin\theta_r, cos\phi)$. When the angle $\phi = \pi/2$ the molecules lie in the plane and the periodicity $\theta \rightarrow \theta + \pi$ must be observed. When they are not in the plane, θ and $\theta + \pi$ are no longer equivalent and a

possible action describing this is

$$A = -K \sum_{\alpha,\beta} \sum_{<rr'>} [n_r^\alpha \, n_r^\beta - n_{r'}^\alpha \, n_{r'}^\beta]^2 \tag{3.4}$$

When the local director n_r is expressed in terms of angles θ_r and ϕ we obtain (3.3) with $\alpha = 4K sin^2\phi cos^2\phi$ and $\beta = K sin^4\phi$, which has the correct limit when $\phi = \pi/2$ and describes a nematic. Depending on the tilt angle ϕ, the transition smectic $\leftrightarrow$ isotropic will take place either directly via an XY transition or through an intermediate nematic (unlocked) phase with an XY followed by an Ising transition as the temperature is lowered. This ignores the possibility of crystallization which may preempt one or both transitions. Unfortunately there is no experimental realization of a two-dimensional nematic because of rupturing of the film.

3.2 Electrodynamic representation for coupled XY models

In order to proceed with the investigation of the critical behavior in the model (3.1), we need to treat vortex excitations explicitly. This can be achieved by transforming the model to an equivalent electrodynamic representation (Kadanoff, 1976). In this representation problems of two-dimensional statistical mechanics can be formulated in terms of two sets of integer variables M_R and S_r which reside on sites $\vec{R}$ of the dual lattice and sites $\vec{r}$ of the original lattice. Interaction between charges of the same kind (the M's for example) at large separations is proportional to the logarithm of the distance between them. The interaction between M_R and S_r, on the other hand, are proportional to the angle between the vector $\vec{R} - \vec{r}$ and some fixed reference direction in the plane. The interaction between M_R and S_r is similar to charges and magnetic monopoles. An interesting property of the coulomb gas representation is that duality transformations for the original model correspond to a simple interchange of charges of the type M_R and S_r.

The main motivation to rewrite the model in a coulomb gas representation is that recursion relations can be obtained by a procedure that is now considered standard (Kosterlitz,

1974; Nelson and Halperin, 1980). In addition to this, the coulomb gas representation unifies various models. The difference between the models are reflected only in changes in the parameters of the interactions between the charges.

First we write the symmetry breaking term as

$$e^{h\cos p(\theta_r - \phi_r)} = \sum_{S_r} e^{ipS_r(\theta_r - \phi_r) + lny_s S_r^2} \tag{3.5}$$

If $y_s \to 0$, only the terms $S = 0$ and $S = \pm 1$ contribute and the left and right-hand side of (3.5) are equal provided $y_s = h/2$. When $y_s \to 1$, $\theta_r - \phi_r$ is forced to take the values

$$\theta_r - \phi_r = \frac{2\pi}{p}\tau_r, \qquad \tau_r = 0, 1, 2 \ \ ..., p-1 \tag{3.6}$$

The equivalent electrodynamic representation of (3.1) is found to be (Appendix B)

$$Z = \left[\prod_r \sum_{S_r}{}'\right]\left[\prod_R \sum_{M_R}{}' \sum_{N_R}{}'\right] e^{\ A(M,N,S)} \tag{3.7}$$

where

$$A(M,N,S) = \pi\alpha \sum_{R,R'} M_R\, G(R-R')M_{R'} + \pi\beta \sum_{R,R'} N_R\, G(R-R')N_{R'}$$

$$+ 2\pi g \sum_{R,R'} M_R\, G(R-R')N_{R'} + pi \sum_r \sum_R S_r\, \Theta(r-R)[M_R - N_R]$$

$$+ \pi\gamma \sum_{r,r'} S_r\, G(r-r')S_{r'} \tag{3.8}$$

and

$$\gamma = \frac{p^2(\alpha + \beta + 2g)}{4\pi^2(\alpha\beta - g^2)} \tag{3.9}$$

The primes on the summation over the three integer fields indicate that they are subject to the neutrality condition

$$\sum_R M_R = \sum_R N_R = \sum_r S_r = 0 \tag{3.10}$$

The large-distance behavior of the Green's functions $G(R-R')$ and $\Theta(r-R)$ are

$$G(R-R') = \ln\frac{|\vec{R} - \vec{r}'|}{a} + \frac{\pi}{2}$$
$$\Theta_r = \tan^{-1}(y/x) \tag{3.11}$$

where $r = (x, y)$. Correlations functions can be treated similarly. The various phases in Figure 3.1 can be distinguished by the large-distance behavior of the correlation functions. The correlation functions $< e^{iq(\theta_\rho - \theta_{\rho'})} >$ and $< e^{iq(\phi_\rho - \phi_{\rho'})} >$, which describe the XY order in each variable, and the cross correlation function $< e^{iq(\theta_\rho - \phi_{\rho'})} >$ can be written in the Coulomb-gas representation as

$$< e^{iq(\theta_\rho - \theta_{\rho'})} > = |\rho - \rho'|^{-q^2\beta/2\pi(\alpha\beta - g^2)} Z^{-1} [\prod_r {\sum_{S_r}}']' [\prod_R {\sum_{M_R}}' {\sum_{N_R}}']' e^{A(M,N,S)}$$

$$\exp\left[iq \sum_R M_R [\Theta(\rho - R) - \Theta(\rho' - R)] \right.$$

$$\left. + \frac{qp(\beta + g)}{2\pi(\alpha\beta - g^2)} \sum_r S_r [G(r - \rho) - G(r - \rho')] \right] \tag{3.12}$$

$$< e^{iq(\phi_\rho - \phi_{\rho'})} > = |\rho - \rho'|^{-q^2\alpha/2\pi(\alpha\beta - g^2)} Z^{-1} [\prod_r {\sum_{S_r}}']' [\prod_R {\sum_{M_R}}' {\sum_{N_R}}']' e^{A(M,N,S)}$$

$$\exp\left[iq \sum_R N_R [\Theta(\rho - R) - \Theta(\rho' - R)] \right.$$

$$\left. + \frac{qp(\alpha + g)}{2\pi(\alpha\beta - g^2)} \sum_r S_r [G(r - \rho) - G(r - \rho')] \right] \tag{3.13}$$

$$< e^{iq(\theta_\rho - \phi_{\rho'})} > = |\rho - \rho'|^{-q^2 g/2\pi(\alpha\beta - g^2)} e^{q^2(\alpha + \beta + 2g)/8(\alpha\beta - g^2)}$$

$$Z^{-1} [\prod_r {\sum_{S_r}}']' [\prod_R {\sum_{M_R}}' {\sum_{N_R}}']' e^{A(M,N,S)}$$

$$\exp\left[iq \sum_R M_R \Theta(\rho - R) - N_R \Theta(\rho' - R) \right.$$

$$\left. + \frac{qp}{2\pi(\alpha\beta - g^2)} \sum_r S_r [(\beta + g)G(r - \rho) + (\alpha + g)G(r - \rho')] \right] \tag{3.14}$$

for integer values of q. The correlation functions (3.12) and (3.13) are not convenient to describe the XY-like behavior of the model in the different regions of the phase diagram.

An appropriate one is

$$< e^{iq[(\theta_\rho+\phi_\rho)-(\theta_{\rho'}+\phi_{\rho'})]} > = |\rho - \rho'|^{-q^2(\alpha+\beta-2g)/2\pi(\alpha\beta-g^2)} \cdot$$

$$Z^{-1}[\prod_r \sum_{S_r}{}'][\prod_R \sum_{M(R)}{}' \sum_{N(R)}{}']e^{A(M,N,S)}$$

$$\exp\left[iq\sum_R (M_R + N_R)[\Theta(\rho - R) - \Theta(\rho' - R)]\right.$$

$$\left. + \frac{qp(\beta-\alpha)}{2\pi(\alpha\beta - g^2)} \sum_r S_r [G(r-\rho) - G(r-\rho')]\right] \qquad (3.15)$$

To describe the long-range order in the locked phase we use the correlation function

$$< e^{iq[(\theta_\rho-\phi_\rho)-(\theta_{\rho'}-\phi_{\rho'})]} > = |\rho - \rho'|^{-q^2(\alpha+\beta+2g)/2\pi(\alpha\beta-g^2)}$$

$$Z^{-1}[\prod_r \sum_{S_r}{}'][\prod_R \sum_{M_R}{}' \sum_{N_R}{}']e^{A(M,N,S)}$$

$$\exp\left[iq\sum_R [(M_R - N_R)\Theta(\rho - R)\right.$$

$$- (M_R - N_R)\Theta(\rho' - R)]$$

$$\left. + \frac{qp(\alpha+\beta+2g)}{2\pi(\alpha\beta - g^2)} \sum_r S_r [G(r-\rho) - G(r-\rho')]\right] \qquad (3.16)$$

3.3 Recursion relations in the weak-coupling limit

In order to remove the short-ranged interactions from the representation (3.8), we need to use an extension of the renormalization-group method for the XY model (Kosterlitz, 1974). The $|R - R'| = a$ and $|r - r'| = a$ terms in (3.8) generate the followings terms

$$\sum_R M_R^2 \ln y_m + \sum_R N_R^2 \ln y_n + \sum_r S_r^2 \ln y_s \qquad (3.17)$$

where

$$\begin{aligned} y_m &= \exp(-\pi^2\alpha/2) \\ y_n &= \exp(-\pi^2\beta/2) \\ y_s &= (h/2)\exp(-\pi^2\gamma/2) \end{aligned} \qquad (3.18)$$

are the fugacities for their respective charges.

There is an additional term $\pi^2 g \sum_R M_R N_R$ that can provide a fugacity associated to hybrid vortices, i.e., configurations in which M vortex and N vortex reside at the same site. The resulting recursion relations are discussed in the Appendix C. For the region of the phase diagram which we discuss next they are irrelevant.

In order to restrict the charges to take only the values 0 and ± 1 we consider only small values of the fugacities. The effect of small y_s is to unlock the variables θ_r and ϕ_r in the action (3.1) and corresponds to h small.

Recursion relations can be derived by a straighforward generalization of the Kosterlitz method (1984) (Appendix C). The fugacity recursion relations can be easily obtained from its scaling behavior when the lattice spacing is increased. We find

$$\begin{aligned} \frac{dy_m}{dl} &= (2 - \pi\alpha) y_m \\ \frac{dy_n}{dl} &= (2 - \pi\beta) y_n \\ \frac{dy_s}{dl} &= (2 - \pi\gamma) y_s \end{aligned} \tag{3.19}$$

where lengths have been scaled by a factor e^l. The coefficient α is renormalized by considering all contributions from the reescaling of the lattice spacing $a \rightarrow a + da$ which are proportional to MGM. Although the detailed calculation of these contributions is complicated, one can obtain the final result in a easy way by considering all contributions proportional to MGM which arise when we contract any neutral pair of the charges. These contributions are $(2\pi\alpha)^2 M \widetilde{GMMG} M$, $(2\pi g)^2 M \widetilde{GNNG} M$ and $(-ip)^2 M \widetilde{\Theta S S \Theta} M$. For the others coefficients the procedure is the same. The corresponding recursion relations are

$$\begin{aligned} \frac{d\alpha}{dl} &= -4\pi^3 \alpha^2 y_m^2 - 4\pi^3 g^2 y_n^2 + \pi p^2 y_s^2 \\ \frac{dg}{dl} &= -4\pi^3 \alpha g y_m^2 - 4\pi^3 \beta g y_n^2 - \pi p^2 y_s^2 \\ \frac{d\beta}{dl} &= -4\pi^3 \beta^2 y_n^2 - 4\pi^3 g^2 y_m^2 + \pi p^2 y_s^2 \\ \frac{d\gamma}{dl} &= -4\pi^3 \gamma^2 y_s^2 + \pi p^2 y_m^2 + \pi p^2 y_n^2 \end{aligned} \tag{3.20}$$

Using Equations (3.9), (3.19) and (3.20) one finds that the recursion relation for γ is consistent with the other three and therefore the relation (3.9) is preserved under renormalization.

By considering the region of the (α, g, β) parameter space for which $\pi\beta > 2$ and using Equation (3.19) it is apparent that the fugacity y_n is irrelevant in this region. This irrelevance allows us to consider $N(R) = 0$ in (3.8). A numerical iteration of (3.19) and (3.20) shows that there is in fact a region in which y_n is irrelevant. The action is consequently simplified to

$$A(M,S) = \pi\alpha \sum_{R.R'} M_R\, G(R-R')M_{R'} + pi \sum_{r} \sum_{R} S_r \Theta(r-R) M_R + \frac{p^2(\alpha+\beta+2g)}{4\pi(\alpha\beta-g^2)} \sum_{r,r'} S_r\, G(r-r')S_{r'} \tag{3.21}$$

It is now possible to exploit the dual symmetry of this action under the transformation $M \leftrightarrow S$. As was shown by Kadanoff (1976), duality transformation in the original model corresponds to the interchange of S by M in the Coulomb gas representation. Usually the phase transition occurs at values of the parameters that make the Action self dual.

For the action in consideration (3.21), provided one chooses $y_m = y_s$, there is a self-dual surface in the (α, g, β) parameter space given by

$$4\pi^2\alpha(\alpha\beta - g^2) = p^2(\alpha+\beta+2g) \tag{3.22}$$

for $p = 2$ and $p = 3$ this must represent the boundary between two low-temperature phases. The renormalization-group recursion relations (3.19) and (3.20) on the self-dual surface $y_m = y_s = y$ now reads

$$\begin{aligned} \frac{dy}{dl} &= (2-\pi\alpha)y \\ \frac{d\alpha}{dl} &= 4\pi y^2(p^2/4 - \pi^2\alpha^2) \\ \frac{dg}{dl} &= -4\pi y^2(p^2/4 + \pi^2\alpha g) \\ \frac{d\beta}{dl} &= 4\pi y^2(p^2/4 - \pi^2 g^2) \end{aligned} \tag{3.23}$$

It is clear from these equations that $\pi\alpha$ will decrease from an initial value greater than $p/2$. It must eventually flow to a line of attractive fixed points somewhere else in the self-dual surface. Assuming that Equations (3.23) are qualitatively true for all values of y, it can be speculated that these fixed points occur for $\pi\alpha = p/2$ and $\pi g = -p/2$ with $y \approx 1$,

independent of β. Therefore the renormalized action must be characterised by a surface in the (α, g, β) parameter space, intersecting the self-dual surface along the line $\pi\alpha = p/2$, $\pi g = -p/2$ with $y_m = y_e \approx 1$.

From Equations (3.23), with $y_n = 0$, it is found that

$$\frac{d}{dl}(\alpha + g) = -4\pi^3 \alpha(\alpha + g) y_m^2 \tag{3.24}$$

This suggests that this surface is given by $\alpha + g = 0$ with $y_m = y_e \approx 1$, in the vicinity of the fixed points.

Using $\alpha + g = 0$ in (3.9) we have $\pi\gamma = p^2/4\pi\alpha$ and the action (3.8) with $N_R = 0$ reduces to

$$A(M, S) = \pi\alpha \sum_{R.R'} M_R G(R - R') M_{R'} + pi \sum_r \sum_R S_r \Theta(r - R) M_R + \frac{p^2}{4\pi\alpha} \sum_{r,r'} S_r G(r - r') S_{r'} \tag{3.25}$$

which is the same action one obtains for a p-state clock model (Elitzur et al, 1979). This indicates that the phase transition is governed by a line of fixed points of Ising character ($p = 2$) or 3-state Potts character ($p = 3$). The same analysis can be performed for the region of the parameter space $\pi\alpha > 2$. By symmetry we then obtain another line of fixed points at $\pi\beta = p/2$ and $y_n = y_e \approx 1$.

In addition to those lines of fixed points we also expect two lines of fixed points along the axis for $\alpha = 0$, $\pi\beta > 2$, and $\beta = 0$, $\pi\alpha > 2$ corresponding to the usual XY line of fixed points for a single XY model. In the limit $\beta \to \infty$, (3.1) reduces to an XY model with symmetry breaking field (José et al, 1977), one then expects an Ising-like and a 3-state-Potts-like transition for $p = 2$ and $p = 3$, respectively. For α near zero, the M vortices are highly relevant and can be integrated out. This procedure leads to an effective $\beta' = \beta - g^2/\alpha$ and the S variables bound together by strings with a linear interaction and therefore irrelevant (see the discussion in Section 3.5). So the transition temperature at finite g should be decreased. The expected pattern of renormalization-group trajectories is indicated in Figure 3.5

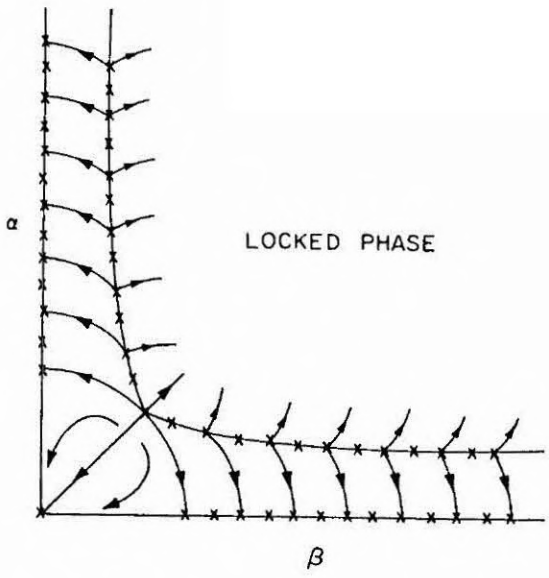

Figure 3.5 Schematic renormalization-group trajectories.

A numerical interation of Equations (3.19) and (3.20) performed until the fugacities are of order 1, confirms Figure 3.5 and gives the phase diagram of Figure 3.1. A distinct point P along the line of initial points $\alpha = \beta$ separates the low- and the high-temperature phases. The locked phase corresponds to a power-law decay of correlations for θ_r and ϕ_r fields, and in this region, fluctuations in θ_r are tied to fluctuations in ϕ_r. Phase B corresponds to Ising-like (p=2) or 3-state-Potts-like (p=3) disorder and XY-like order in the field ϕ_r and it is separated from the locked phase by an Ising (p=2) line PB. Phase A corresponds to the analogous behavior for the field θ_r. Both phases in turn are separated from the high-temperature phase corresponding to Ising disorder and XY disorder by the line CPD. We are unable to determine in which precise form the two lines meet at the point P, although the flows are consistent with the topology indicated in the inserts A and B of Figure 3.1.

The difference between our model and the p-state clock model transition along the line APB lies in the behaviour of the correlation functions. If $\alpha + g = 0$ and $N(R) = 0$ the expression (3.12) reduces to

$$< e^{iq[\theta_\rho - \theta_{\rho'}]} > = |\rho - \rho'|^{-q^2\eta} F_p^q(\rho - \rho') \tag{3.26}$$

Here $F_p^q(\rho - \rho')$ is the corresponding correlation function for the p-state clock model (Elitzur

where h_r is the new integer field introduced by the Poisson formula.

Integrating freely over ϕ_r and using the identity $\sum_{r'} G^{-1}_{rr'} G_{r'r''} = \delta_{rr''}$ we obtain (up to constant factors)

$$I = |\vec{\rho} - \vec{\rho'}|^{-\frac{A^2 BC}{2\pi^2\gamma}} \left[\prod_r \sum_{h_r}\right] \exp\left[-\frac{1}{\pi\gamma}\sum_r h_r G^{-1}_{rr'} h_{r'} + i\frac{A}{\pi\gamma}(Ah_\rho + Ch_{\rho'})\right]$$

where we made use of the large distance behavior of $G_{rr'}$ (Equation B.7). By definition

$$\sum_{r,r'} h_r G_{rr'} h_{r'} = \sum_{<rr'>} (h_r - h_{r'})^2$$

We can then recognize the second term in (D.3) as a particular correlation function of the roughening model discussed in Section 2.4.2 (Equation 2.44 with $f = 0$). For the region of the phase diagram $\pi\alpha > 2$, $\pi\beta > 2$, we have $\pi\gamma << 1$. This corresponds to a low temperature for the roughening model. Since at low temperatures one expects a long range order the second factor in (D.3) approaches a constant when $|\vec{\rho} - \vec{\rho'}| \to \infty$ and (D.5) reduces to a pure power law behavior. When this result is substituted in Equations 3.12 - 3.16, we obtain for $|\rho - \rho'| \to \infty$

$$\begin{aligned} &< e^{iq[\theta_\rho - \theta_{\rho'}]} > = |\rho - \rho'|^{-q^2\eta} \\ &< e^{iq[\phi_\rho - \phi_{\rho'}]} > = |\rho - \rho'|^{-q^2\eta} \qquad (3.33) \\ &< e^{iq[\theta_\rho - \phi_{\rho'}]} > = |\rho - \rho'|^{-q^2\eta} \end{aligned}$$

and

$$< e^{iq[(\theta_\rho + \phi_\rho) - (\theta_{\rho'} + \phi_{\rho'})]} > = |\rho - \rho'|^{-4q^2\eta} \qquad (3.33a)$$

$$< e^{iq[(\theta_\rho - \phi_\rho) - (\theta_{\rho'} - \phi_{\rho'})]} > \to const \qquad (3.33b)$$

with $\eta = \frac{1}{2\pi(\alpha + \beta + 2g)}$

Therefore in this region the correlation functions (3.32) and (3.33a) decay algebraically and are characterized by the same renormalized constant η while long range order is reflected in the correlation function (3.33b). The corresponding phase is locked. Although this analysis was performed for the region $\pi\alpha > 2$ and $\pi\beta > 2$, the Migdal renormalization-group analysis to be discussed later, suggests that the low-temperature side of the line APB

et al, 1979) with $F_p^p = 1$ and

$$\eta = \frac{1}{2\pi(\beta - \alpha)} \tag{3.27}$$

for the field ϕ_r we similarly find

$$< e^{iq[\phi_\rho - \phi_{\rho'}]} > = |\rho - \rho'|^{-q^2\eta} \tag{3.28}$$

Near the line PB the correlation function $F_p^{q=1}(\rho - \rho')$ approaches a constant or decays exponentially to zero as $|\rho - \rho'| \to \infty$ if we are above or below this line, respectively. It follows that for phase A

$$\begin{aligned} < e^{i[\theta_\rho - \theta_{\rho'}]} > &= |\rho - \rho'|^{-\eta_A(\alpha, g, \beta)} \\ < e^{i[\phi_\rho - \phi_{\rho'}]} > &= |\rho - \rho'|^{-\eta_A(\alpha, g, \beta)} e^{-|\rho - \rho'|/\xi} \end{aligned} \tag{3.29}$$

where ξ is the correlation length of the p-state clock model. Similarly, for phase B

$$\begin{aligned} < e^{i[\phi_\rho - \phi_{\rho'}]} > &= |\rho - \rho'|^{-\eta_B(\alpha, g, \beta)} \\ < e^{i[\theta_\rho - \theta_{\rho'}]} > &= |\rho - \rho'|^{-\eta_B(\alpha, g, \beta)} e^{-|\rho - \rho'|/\xi} \end{aligned} \tag{3.30}$$

Note that for $q = p$, all correlation functions are algebraic in all ordered phases. In the high temperature phase all correlation functions decay exponentially.

In the region where $\pi\alpha > 2$ and $\pi\beta > 2$, we can take $M(R), N(R) = 0$. In this region $S(r)$ is relevant. Nevertheless, one can transform Equations 3.12 - 3.16 to another representation with the corresponding integer fields dilute in that region using the Poisson summation formula (2.45). With $M_R = N_R = 0$, the term involving summations in S_r in equations 3.12 - 3.16 can be written as

$$I = \left[\prod_r \sum_{S_r}\right] \exp\left[- 2\pi^3\gamma \sum_{r,r'} S_r G_{rr'} S_{r'} + 2\pi A \sum_r S_r (BG_{r\rho} + CG_{r\rho'}\right] \tag{3.31}$$

where $G_{rr'}$ is the lattice Green's function defined in Equation (B.6).

Using (2.45) the above expression can be written as

$$I = \left[\prod_r \sum_{h=-\infty}^{\infty}\right] \int_{-\infty}^{\infty} d\phi_r \exp\left[- 2\pi^3\gamma \sum_{r,r'} \phi_r G_{rr'} \phi_{r'} + 2\pi \sum_r \phi_r (ABG_{r\rho} + ACG_{r\rho'} - ih_r)\right] \tag{3.32}$$

is all locked and the behavior described by (3.32) and (3.33) extends thoroughout the region. In the unlocked phases A and B standard arguments imply that $0 < \eta_{A,B} < \frac{1}{4}$, the upper value being reached on the phase boundaries between the partially ordered and completely disordered phases.

Because of the form of the fourth term in the action (3.8), one would be inclined to perform a change of variable such as $M_R - N_R \rightarrow L_R$ and $M_R \rightarrow K_R$, in which case one obtains

$$A(K,L,S) = \pi\alpha_2 \sum_{R,R'} K_R\, G(R-R')K_{R'} + \pi\beta_2 \sum_{R,R'} L_R\, G(R-R')L_{R'}$$

$$+ 2\pi g_2 \sum_{R,R'} K_R\, G(R-R')L_{R'} + pi \sum_{r} \sum_{R} S_r\, \Theta(r-R)L_R$$

$$+ \pi\gamma_2 \sum_{r,r'} S_r\, G(r-r')S_{r'} \tag{3.34}$$

where $\alpha_2 = \alpha + \beta + 2g$; $\beta_2 = \beta$ and $g_2 = -\beta - g$ are the initial values of the coupling parameters. γ_2 ca be written in terms of α_2, β_2 and g_2 as $\gamma_2 = \frac{p^2\alpha_2}{4\pi^2(\alpha_2\beta_2 - g_2^2)}$. Performing the same analyses as before, we find that a fixed point occur along the $\alpha = \beta$ line when $g_2^* = 0$. This is a very interesting result since it implies that the XY transition (represented by the M vortices) and the Ising transition (due to the M, S vortices) happen independently. This possibility is suggested by the numerical work of Lee et al (1986) on the antiferromagnetic XY model on a triangular lattice. They found that that the numerical simulation is consistent with a simultaneous XY and Ising transition.

We show in Appendix C, however, that when hybrid vortices made up of a K and L of opposite signs are included, g_2 does not renormalize to zero and the K and L charges do not decouple. In fact, if we identify K as a hybrid vortex of M and N in (3.8) and L as the N vortices, then the hybrid made up of L and K is the M vortex in (3.8). When hybrid vortices are included in the recursion relations derived from (3.34) we obtain the recursion relations obtained from the action (3.8). This is not surprising since, after all, (3.34) was obtained by a simple change of variables.

3.4 Strong-coupling limit and the Migdal recursion relations

The analysis of the preceding sections shows that in the locked phase y_s is relevant; this corresponds to $h \to \infty$ in (3.1). In this limit $\theta_r - \phi_r$ assumes the values given by (3.6). For $p = 2$ one can define the Ising variables $S(r) = 2\tau(r) - 1$ and obtain

$$A = \beta \sum_{<rr'>} \cos(\phi_r - \phi_{r'}) + \alpha \sum_{<rr'>} S_r S_{r'} \cos(\phi_r - \phi_{r'}) \tag{3.35}$$

This action will describe the critical behavior associated to the field ϕ_r. We can investigate the phase diagram of this model by using an approximate position-space renormalization group transformation introduced by Migdal (1975). Here we apply this transformation in a form due to Kadanoff (1976).

First we need to consider a more general form of the action (3.35):

$$A = \sum_{<rr'>} V(\phi_r - \phi_{r'}) + \sum_{<rr'>} S_r S_{r'} F(\phi_r - \phi_{r'}) + L \sum_{<rr'>} S_r S_{r'} \tag{3.36}$$

where $V(\phi)$ and $F(\phi)$ are periodic functions with period 2π. The original expression (3.35) is recovered upon setting $V(\phi) = \beta cos\phi, F(\phi) = \alpha cos\phi$, and $L = 0$. The additional term has to be included since the form (3.35) is not preserved under renormalization. To apply the Migdal transformation one first moves bonds on the lattice such that the sites to be integrated out at each stage are linked to their neighbors only in one spacial direction. This bond moving allow us to perform a one-dimensional decimation to obtain an effective interaction between the remaining degrees of freedom.

In terms of $u(\phi) = e^{V(\phi)-V(0)}, z = e^{F(0)+L}$ and $f(\phi) = e^{F(\phi)-F(0)}$ the parameters (primed) of the new Hamiltonian are therefore given by the recursion relations

$$\begin{aligned}
z'^2 &= \frac{z^4 A_1(0) + z^{-4} A_4(0)}{A_2(0) + A_3(0)} \\
u'^2(\phi) &= \frac{[A_2(\phi) + A_3(\phi)][z^4 A_1(\phi) + z^{-4} A_4(\phi)]}{[A_2(0) + A_3(0)][z^4 A_1(0) + z^{-4} A_4(0)]} \\
f'^2(\phi) &= \frac{[A_2(0) + A_3(0)][z^4 A_1(\phi) + z^{-4} A_4(\phi)]}{[z^4 A_1(0) + z^{-4} A_4(0)][A_2(\phi) + A_3(\phi)]}
\end{aligned} \tag{3.37}$$

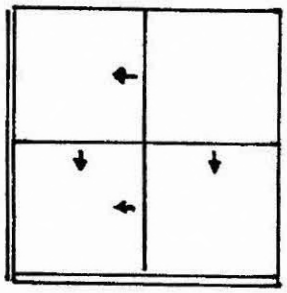

Figure 3.6 Bond moving for a two dimensional square lattice. New vertical and horizontal bonds are obtained by moving any other vertical and horizontal bond on top of a remaining bond. New bonds are then obtained by integrating out the isolated vertices.

where

$$
\begin{aligned}
A_1(\phi) &= \int_0^{2\pi} \frac{d\theta}{2\pi} u^2(\theta) u^2(\theta-\phi) f^2(\theta) f^2(\theta-\phi) \\
A_2(\phi) &= \int_0^{2\pi} \frac{d\theta}{2\phi} u^2(\theta) u^2(\theta-\phi) f^{-2}(\theta) f^2(\theta-\phi) \\
A_3(\phi) &= \int_0^{2\pi} \frac{d\theta}{2\pi} u^2(\theta) u^2(\theta-\phi) f^2(\theta) f^{-2}(\theta-\phi) \\
A_4(\phi) &= \int_0^{2\pi} \frac{d\theta}{2\pi} u^2(\theta) u^2(\theta-\phi) f^{-2}(\theta) f^{-2}(\theta-\phi)
\end{aligned}
\tag{3.38}
$$

A numerical iteration of Equations (3.37) gives a phase diagram similar to Figure 3.1. The line APB separates the low-temperature region where $L \to \infty$ (Ising order) from the regions B and A where $L \to 0$ (Ising disorder). In this Figure the axial parameters are now defined by $\alpha_{e\alpha} = -\frac{1}{2} \ln f(\pi)$ and $\beta_{e\alpha} = -\frac{1}{2} \ln u(\pi)$. They reduce to α and β, respectively, for the initial values $u(\phi) = e^{\beta \cos\phi - \beta}$ and $f(\phi) = e^{\alpha \cos\phi - \alpha}$. Actually, one should observe the evolution of the functions $u(\phi)$ and $f(\phi)$ in the whole interval $0 < \phi < 2\pi$, but the

above defined parameters provide a convenient way of following the renormalization flows. Above and below the line PB, after a few iterations, $f(\phi) \to 1$ and $u(\phi)$ relaxes to a Villain potential (Villain, 1975). Unfortunately the Migdal transformation does not actually lead to a fixed line and a small drift toward higher temperatures is always present (José et al, 1977). Therefore the line CD separating the disordered high-temperature phase from the fixed line $\beta > \beta_D$ cannot be precisely determined.

The line APB corresponds to Ising-like transition. In fact for $\beta > \alpha$, $f(\phi)$ and $u(\phi)$ renormalize to $f'(\phi) = 1$ and $u'(\phi) = u^*(\phi)$. Using the recursion relations (3.37) we find $\delta L' = e^{\lambda \ln 2} \delta L$, where $\delta L'$ and δL are the deviations from the fixed point and $\lambda = 0.74$. This is the same result one finds for the two-dimensional Ising model using the same approximation.

Near the point P, however, we cannot estimate the critical exponents due to the drift to high temperatures in the Migdal approximation. Again we cannot determine the way the two lines join or the kind of transition at that particular point. It is apparently consistent with a single transition but if two successive transitions do in fact occur the Migdal approximation then indicates they are very close together with an XY transition followed by an Ising transition as temperature is increased. In particular we find that the region above the Ising line PB is a locked phase with power-law decay of correlations. Although we have studied the limit $h \to \infty$ for the case $p = 2$, we also expect similar results for $p = 3$, where instead of an Ising we would have a 3-state Potts transition (Choi and Doniach, 1985).

3.5 Linear and logarithmic interacting vortices

In the model (3.1) , vortex excitations can appear as a result of the continuous symmetry of the action in both θ_r and ϕ_r fields. Not all the ground states can be connected by a continuous transformation and the ground state has a discrete degeneracy. A domain wall excitation therefore separates a ground-state configuration corresponding to $\theta_r - \phi_r = 0$ from another nonequivalent ground state $\theta_r - \phi_r = 2\pi/p$.

The energy of an isolated vortex is proportional to $\ln L$, where L is the linear dimen-

sion of the system. Therefore one expects logarithmic interacting vortex pairs of opposite vorticities at low temperatures. Since the entropy of such a pair is also proportional to $\ln L$, they can unbind at some higher temperature.

On the other hand, since there is a change of phase of $2\pi/p$ when crossing a domain wall, one can also produce a vortex by joining to the same point the ends of p domain walls (Einhorn et al, 1980). The energy of such a vortex is proportional to the linear dimension of the system because a domain wall has a finite energy per unit length. Therefore, at low temperatures one expects they are connected by strings (domain walls) in pairs of opposite vorticities. This linear interaction suppresses an XY-like unibinding.

In the locked phase y_s is strongly relevant. one can now transform (3.8) into another representation where the corresponding integer fields are dilute in that regime using (2.45). The necessary manipulations are described in Heinekamp and Pelcovits (1985). Dropping an overall constant factor, we get

$$Z = \left[\prod_R {\sum_{M_R}}' {\sum_{N_R}}'\right] e^{A(M,N)} \tag{3.39}$$

where

$$\begin{aligned} e^{A(M,N)} = \exp\Bigg[& \pi(\alpha - \frac{p^2}{4\pi^2\gamma}) \sum_{R,R'} M_R\, G(R-R')M_{R'} \\ & + \pi(\beta - \frac{p^2}{4\pi^2\gamma}) \sum_{R,R'} N_R\, G(R-R')N_{R'} \\ & + 2\pi(g + \frac{p^2}{4\pi^2\gamma}) \sum_{R,R'} M_R\, G(R-R')N_{R'} \Bigg] \\ & \times \left[\prod_r \sum_{h_r}\right] \exp\left[-\frac{1}{2\gamma} \sum_{<rr'>} [h_r - h_{r'} - p\sum_R \eta_{rr'}(R)(M_R - N_R)]^2 \right] \end{aligned} \tag{3.40}$$

$\eta_{rr'}(R)$ is the operator introduced by José et al (1977), it is $+1$ if r lies just to the right and r' just to the left of an arbitrary path going from R to ∞ in the positive x direction, -1 if r and r' are reversed, and 0 otherwise.

The first three terms in (3.40) represent logarithmic interacting vortices now corrected by a term $p^2/4\pi^2\gamma$ due to domain walls. The last term corresponds to the partition function for a set of domain walls of strengh p running from R to R' in the roughening model (Swendsen, 1978). Thus this term represents vortex pairs interacting linearly and connected by p domain walls of unit strengh. The interaction energy for a vortex pair has therefore two contributions: a logarithmic and a linear distance dependence. If the strings have not melted these vortex pairs interact linearly for large distance separations and an XY-unbinding transition is suppressed. However when the strings melt these vortices interact logarithmically, as can be seen by replacing the sum of the integers h_r by an integral over a continuous field. The corresponding phase now depends on the behavior of these vortices. The M vortices would unbind for $\pi\alpha < 2$ and the N for $\pi\beta < 2$. If the melting of the domain walls occurs inside these regions the relevant vortex pair will unbind at that temperature and disorder the corresponding field.

From (3.40) we can identify the free energy per unit length (divided by $k_B T$) of a domain wall as $\frac{1}{2\gamma}$ when $T \to 0$. Using a Peierls argument to determine when the free energy of a domain wall goes to zero we obtain that the string melting occurs at temperatures given by $\gamma = \frac{1}{2ln3}$. This gives melting curves similar to APB in Figure 3.1 When $g = 0$, this curve intersects the region where $\pi\alpha < 2$ and $\pi\beta < 2$ only for $p = 2$.

However, the effect of a renormalized $g < 0$ is to move these lines further inside that region. In particular, for $g = -\alpha$ along the line $\alpha = \beta$, the $p = 3$ melting curve also intersects this region but $p = 4$ curve does not. Thus we expect that that for $p = 2$ and $p = 3$ there is no intermediate phase with XY order and p-state clock disorder (p=2,3) and we are left with the two possibilities indicated in Figure 3.1.

On the $\alpha = \beta$ line, which is, of course, the most interesting from an experimental point of view, the weak coupling recursion relations do not say very much because one can construct a large number of relevant operators. In particular the M, N and S charges are all relevant with increasing fugacities. Also, the hybrid vortices with $M_R = N_R$ on the same

site are highly relevant, while the hybrid vortices with $M_R = -N_R$ are irrelevant and will be ignored now on. Now at large α the M, N and H vortices are irrelevant but y_s is strongly relevant which when integrated out gives the string picture. When the temperature is increased (α decreased) although the recursion relations (3.19) seem to indicate that the M and N vortices are relevant they are still bound together by strings. The hybrid vortices are not bound by strings as can be verified by Equations (3.40). So the important configurations are: (i) a pair of $M(N)$ vortices of opposite signs bound by strings well separated from any other $N(M)$ vortices; (ii) one M and one N vortex of the same sign close together bound by string which can be regarded as a hybrid (H) vortex with a core size of the order of their separation.

These extended objects interact logarithmically with each other on length scales large compared to their size. The separation of the M and N of the same sign can be interpreted as the core size of a hybrid vortex. For $p = 2$ and 3, simple estimates for the sequence of transitions temperatures give $T_M < T_S < T_H$, where T_M is the unbinding temperature of M or N vortices, T_S is the string melting temperature, an T_H is the hybrid vortex unbinding temperature. The M vortices are bound by p strings so the transition in the absence of hybrid vortices would be in the p-state universality class by the string melting. However, the hybrid vortices are screened at $T > T_S$ by the M and N vortices so that they must unbind when the M and N do. Below T_S the M and N vortices are bound for separations less than ξ_p, the correlation length of the p-state model, which can be interpreted as the core size of a hybrid vortex. Thus, in the presence of hybrid vortices, the XY order is lost by the divergence of the hybrid vortex core size which leads one to expect a first-order transition. Note that this picture is fairly close to that by Halsey (1985b) as discussed in Section 2.5. Furthermore, this picture gives an explanation of the mixed p state and XY character of the system as one approaches the transition provided it is rather weakly first order.

These arguments can be applied to the same model with $p = 1$ which is the Villain

representation of the double-layer XY model (Parga and Himbergen, 1980). However the sequence of transition temperatures is $T_M < T_H < T_S$. So this scenario means that the M and N vortices remain bound by strings and the transition is controlled entirely by the hybrid vortices leading to the expected XY transition.

Unfortunately, there is no evidence for such a first-order transition from the extensive Monte Carlo simulations performed on this and related models (Teitel and Jayaprakash, 1983b; Lee et al, 1986; Berge et al, 1986) in 80×80 systems which indicate a transition of mixed Ising and XY character. However, because the unit cell in the triangular antiferromagnet is $\xi_o = \sqrt{3}a$ and in the frustrated XY model on the square lattice $2a$, the largest correlation length is about 30 unit cells long. So there is no sign of a frist-order transition up to $\xi/\xi_o \approx 30$ and so the transition is at best weakly first order.

3.6 Competing periodicities

We turn now to a brief analysis of the XY model with competing periodicities described by (3.2) in the coupled XY model representation (3.3). This representation can be obtained by a Hubbard-Stratonovich transformation as we show next. A related model was discussed by Lee and Grinstein (1985).

First we rewrite the partition function associated with (3.2) as

$$Z = \left[\prod_r \int_0^{2\pi} d\theta_r\right] \exp\left[\frac{1}{2}\sum_{r,r'} e^{-i\theta_r} P_{rr'} e^{i\theta_{r'}} + \frac{1}{2}\sum_{r,r'} e^{-ip\theta_r} Q_{rr'} e^{ip\theta_{r'}}\right] \tag{3.41}$$

Where $P_{rr'} = \alpha_{rr'} + K_P\delta_{rr'}$ and $Q_{rr'} = \beta_{rr'} + K_Q\delta_{rr'}$ with $\alpha_{rr'} = \alpha$, $\beta_{rr'} = \beta$ when r and r' are nearest neighbors and zero otherwise. Here, K_P and K_Q are appropriate constants introduced to make the matrices positive definite. Applying the identity (2.55) separately to the two terms of (3.41), we obtain

$$Z = \left[\prod_r \int_r dx_r \int_r dz_r\right] \exp\left[-\frac{1}{2}x_r^* P^{-1}_{rr'} x_{r'} - \frac{1}{2}z_r^* Q^{-1}_{rr'} z_{r'} - \sum_r H(x_r, z_r)\right] \tag{3.42}$$

where

$$H(x_r, z_r) = -\log\left[\int_0^{2\pi} d\theta \exp[\frac{1}{2}(x_r e^{-i\theta} + x_r^* e^{i\theta}) + \frac{1}{2}(z_r e^{-ip\theta} + z_r^* e^{ip\theta})]\right] \tag{3.43}$$

We can compute from (3.43) the first few low order terms contributing to the free energy. For example, for $p = 2$ we find

$$H(x_r, z_r) = \frac{1}{2}(|x_r|^2 + |z_r|^2) - u(|x_r|^2 + |z_r|^2)^2 - v|x_r|^2|z_r|^2 - w|x_r|^2|z_r|\cos(2\theta - \phi) + O(6) \quad (3.44)$$

In the last term, θ and ϕ are the phases associated with x_r and z_r respectively. The quadratic forms in (3.42) can be diagonalized using Fourier transforms. In a square lattice we have $P(q) = 2\alpha(\cos q_x a + \cos q_y a)$, $Q(q) = 2\beta(\cos q_x a + \cos q_y a)$ which reach a maximum at $q = 0$. Expanding about $q = 0$, the second order terms in (3.42) can be approximated by a continuum form

$$\begin{aligned}\sum_q (P(q)^{-1} - \frac{1}{2})|x_q|^2 &= \sum_q (r + eq^2)|x_q|^2 \\ &= \int d^2 r (r|x_r|^2 + e(\nabla x_r)^2) \end{aligned} \quad (3.45)$$

and similarly for the $|z_r|^2$ terms. As discussed in Section 2.4, in two dimensions the phase transition occurs well below the mean field transition temperatures where fluctuations in the amplitude are irrelevant. Considering fixed amplitudes, from (3.42) and (3.45) we obtain the representation (3.3) where α and β in this expression are proportional to $|x_r|^2$ and $|z_r|^2$ respectively.

The electrodynamic representation of the action is found, by the methods of Section 3.2 to be

$$\begin{aligned} A(M, N, S) = {} & \pi\alpha \sum_{R,R'} M_R G(R - R') M_{R'} + \pi\beta \sum_{R,R'} N_R G(R - R') N_{R'} \\ & + 2\pi g \sum_{R,R'} M_R G(R - R') N_{R'} + i \sum_r \sum_R S_r \Theta(r - R)[pM_R - N_R] \\ & + \pi\gamma \sum_{r,r'} S_r G(r - r') S_{r'} \end{aligned} \quad (3.46)$$

where

$$\gamma = \frac{(\alpha + p^2\beta + 2pg)}{4\pi^2(\alpha\beta - g^2)} \quad (3.47)$$

The analysis is almost identical and we find a self-dual surface when the N vortices are irrelevant given by $\alpha = \gamma$ which corresponds to a p-state transition. The renormalization-group equations on this surface seem to flow to the fixed point at $\pi\alpha = p/2$ and $\pi g = -1/2$

independent of β. Identical arguments to Section 3.5 show that this is a string melting transition between the fully and partially ordered phases of Figure 3.4. The other self-dual line at small values of β does not correspond to a phase transition since it is the XY model in a magnetic field. The representation in terms of vortices and strings is similar to (3.40). The N vortices however are now connected by a single domains wall. These are the equivalent of the half-integer vortices discussed in connection with the model (3.2). The phase diagram is sketched in Figure 3.4 in which phase A is a locked phase and phase B is a partially ordered unlocked phase. The nature of the multicritical point P cannot be determined by these methods although applying the arguments of the previous Sections indicate that there is a first-order segment on the line CP in the neighborhood of P. Note that this p-state transition is not a consequence of an extra Z_p symmetry in the Hamiltonian, but simply due to extra minima in the action for $\alpha < 4\beta$.

Chapter 4

QUENCHED DISORDER IN SUPERCONDUCTING ARRAYS

4.1 Introduction

Although an ordered array of superconducting elements minimizes the effects of disorder, some is inevitably present and one should include these effects when studying the behavior of the system. Weak disorder is irrelevant to the critical behavior of the XY model which corresponds to the zero field case and is also expected to be irrelevant in finite field provided the disorder does not couple to the field. Two kinds of disorder that we show to be relevant to the critical behavior are: a) variations in the area of the superconducting elements of the array which is presumably least serious in the IBM arrays studied by Voss and Webb (1982) and Webb et al (1983) and most serious in the arrays of superconducting squares studied by Tinkham et al (1983) and Kimhi et al (1984); b) randomness in the positions of the nodes or superconducting grains of the array which will certainly be always present. The first leads to uncorrelated variations in the area of each plaquette provided the penetration depth in the grain is small compared to the grain size and hence to random variations in f and the second to highly correlated variations in the flux per plaquette.

In this chapter we present a simple model of a Josephson junction array in a transverse magnetic field with disorder (Granato and Kosterlitz, 1986c). We map the model into a coulomb gas of fractional charges perturbed by a quenched distribution of random charges in the uncorrelated random area situation and, in the random position case, a random distribution of dipoles.

As in the uniformly frustrated model, the behavior at rational values of f is difficult to

ascertain. However, if we restrict ourself to integer values of f, which corresponds to consider the lower envelope of the resistance as a function of f, some more definitive conclusions can be obtained. In this case the model reduces to a coulomb gas of integer charges perturbed by the random distribution of charges or dipoles. In the former we found that there is no superconducting phase for any finite field but there is a remnant of it provided the disorder is small enough. In the latter case, a reentrant phase exist at low temperatures for values of the magnetic field less than some disorder dependent critical value. For larger values and higher temperatures there is no superconducting phase.

These results have direct experimental consequences. There is no published experimental data which may test the prediction for the random plaquette area case. We expect this to be valid for arrays of lead squares since there is bound to be randomness in the individual square sizes. But in these arrays the junction size is quite large and $T_c(H)$ will itself decrease as H^2 in a non-random array. The results for the positional disorder seems to have some experimental support. For magnetic fields larger than the predicted critical value, the resistance should increase slowly and at higher field one expects that this will cross-over to the usual flux-flow resistance $R(H) \propto H$. This seems to be in qualitative agreement with the experiments by Webb et al (1983). However the experimental data is also complicated by oscillations in the lower envelope of resistance which are outside this simple model. In Chapter 5, we propose an interpretation of these oscillations based on the existence of two fundamental areas which can lead to oscillations of two different periodicities.

The reentrant transition predicted for the positional disorder has not been observed experimentaly, but this will not be an easy effect to observe. One also has to consider that the inclusion of charging effects in a non-random array also leads to a reentrant transition (José, 1984).

The kinds of disorder considered here correspond to quenched disorder which implies that one must average the logarithm of the partition function over the random distribution

to produce the free energy, i.e.

$$F = -k_B T [\ln Z(f)]_d \tag{4.1}$$

where $[\quad]_d$ means an average over the randomness.

4.2 Random plaquette area

Provided the transverse penetration depth $(O(\mathring{A}))$ for the grains is less than the grain size $(O(\mu m))$, randomness in the shape of the grains will induce a randomness in the number of flux quanta per plaquette $f = HS/\Phi_o$ through the change in the area. If the field penetrates homogenously the array, the flux in each unit cell will be the same regardless the change in the shape. However the above effect will always be present but to a smaller degree even when the penetration depth is comparable with the grain size because there is a tendency for the field to be excluded via a partial Meissner effect and there will be more flux going through a large than a small area between the grains.

We assume that the areas are gaussianly randomly distributed about some mean a_o^2. Since $f = HS/\Phi_o$, the distribution for the f is given by

$$P(f_R) \propto \exp\left[-\frac{\Phi_o^2}{2H^2\Delta^2}(f_R - f_o)^2\right] \tag{4.2}$$

where Δ^2 is the variance of the area distribution.

The frustrated XY model (2.5) with the above random distribution is similar to a description of spin glass suggested by Hertz (1978). He has shown that this kind of randomness is relevant below 4 dimensions and the $f = 0$ fixed point is completely unstable to this kind of disorder.

In the coulomb gas representation (2.46), the random distribution (4.2) correspond to a coulomb gas of fractional charges perturbed by a random distribution of charges. As mentioned in Section 4.1, we are concerned here mainly with the effect of this kind of disorder in the resistance minima where f_o is an integer. In this case we can shift $M_R \rightarrow M_R + f_o$, so that now we have the problem of a set of integer charges in a background of random

charges with mean zero. Consider a test charge in a region of size L. Since the fluctuation of a random charge at the dual site $\vec{R}$ is $(\delta f_R)^2 = \frac{H^2\Delta^2}{\Phi_o^2}$, the fluctuation of random charges in the region of size L produce a total charge $\frac{H\Delta L}{\Phi_o}$. When this region is chosen of size larger than $\xi = \frac{\Phi_o}{H\Delta}$ the test charge will be completely neutralized by this random fluctuation. Thus charges separated by distances larger than ξ will be unbound. This argument is the converse of that used by Kosterlitz and Thouless (1973). They argued that if charges are unbound, the average total charge in a region of size L is proportional to L while if they are bound in dipoles it is proportional to $L^{1/2}$. Since the present argument leads to a total charge proportional to L, we conclude that there is no screening. We can now identify ξ as the correlation length of the free vortices contributing to the resistance of the array. This indentification also implies a scaling behavior for the correlation length as

$$\xi \sim \Delta_f^{-1} \tag{4.3}$$

where $\Delta_f = H\Delta/\Phi_o$ is the standard deviation of the random distribution of the f. This result is in agreement with that obtained by Ritala (1984) in $d = 4 - \epsilon$ dimensions. Using the arguments of Section 2.3.2, the resistance is given by $R(H) \propto \xi^{-2}$, then

$$R(H) \sim H^2 \tag{4.4}$$

and the resistance will oscillate with a period corresponding to one flux quanta per mean area and the lower envelope of the resistance will rise quadratically for small H. These arguments are low temperature ones and lead one to expect quadratic increase in the resistance at temperatures well below the critical temperature of the corresponding pure model.

4.3 Positional disorder

In the limit where the grain sizes are small relative to the areas between grains or a network of superconducting wires of constant or very small cross section interpersed with weak links, another source of disorder is in the positions of the nodes of the network. The effect of this type of disorder can be easily seem qualitatively. Suppose that a superconducting wire

separating two areas is displaced from its ideal position, increasing one area and decreasing the other. This intuitively leads to two equal and opposite neighboring charges in the equivalent coulomb gas representation or to a quenched distribution of random dipoles. The same will happen for a displacement of the nodes of the array.

We now introduce positional disorder which consists in allowing displacements of the sites from their average position $\vec{r}$ by an amount $\vec{u}_r$ with a probability distribution

$$P(\vec{u}_r) \propto \exp\left[-\frac{1}{2\Delta^2}\vec{u}_r^2\right] \tag{4.5}$$

In practical systems this kind of disorder will induce disorder in the couplings between nodes $J_{r,r'}$. However, we show that small disorder of this kind is irrelevant along the fixed line of the XY model. In order to show this, we have to perform the average over the randomness in (4.1). This free energy can be averaged using the replica trick (Edwards and Anderson, 1975), which makes use of the mathematical identity

$$\left[\frac{F}{k_B T}\right]_d = \left[\lim_{n\to 0}\frac{1-Z^n}{n}\right]_d \tag{4.6}$$

Assuming that the limit process $n \to 0$ and the average over the randomness commute, we can first integrate over the randomness and then take the limit $n \to 0$ at the end of the calculation.

Consider the Hamiltonian (2.5) at integer f in the spin wave aproximation

$$\frac{H}{k_B T} = \frac{1}{2}(K_o + \delta K)\int d^2\vec{r}(\vec{\nabla}\theta)^2 \tag{4.7}$$

and assume that the distribution for the variable δK is

$$P(\delta K) \propto exp\left[-\frac{1}{2\Delta^2}\int d^2\vec{r}(\delta K)^2\right] \tag{4.8}$$

Applying the replica trick, we find a replicated Hamiltonian

$$\frac{H}{k_B T} = -\ln(Z^n) = \frac{1}{2}K_o\int d^2\vec{r}\sum_{\alpha=1}^{n}(\vec{\nabla}\theta_\alpha)^2 + \frac{1}{8}\Delta^2\int d^2\vec{r}\sum_{\alpha,\beta}(\vec{\nabla}\theta_\alpha)^2(\vec{\nabla}\theta_\beta)^2 \tag{4.9}$$

where α and β are replica indices. The last term in (4.9) is clearly irrelevant along the gaussian fixed line because it involves four powers of the gradient operator. Under a length reescaling Δ iterates to zero. This does not apply to granular superconductors because in this case the disorder is very large and presumably dominates the behavior (see for example Goldman and Wolf, 1984). From now on, we assume the coupling $J_{rr'} = J$, a constant.

In order to determine the effect of positional disorder defined by (4.5) in the critical behavior of the frustrated XY model, consider the coulomb gas representation (2.46). Positional disorder will induce a change in the areas of the plaquettes. If we take a continuum limit of the lattice model, we do not distinguish between a lattice point $\vec{r}$ in the original lattice and a lattice point $\vec{R}$ in the dual lattice. In this case the change in the area of a given plaquette is aproximately $S \sim S_o + S_0 \vec{\nabla}_R \cdot \vec{u}_R$ where S_0 is the area of the plaquette in the undisplaced lattice. Since $f = HS/\Phi_o$, this gives

$$f = f_o + f_o \vec{\nabla}_R \cdot \vec{u}_R \tag{4.10}$$

To be consistent with this linear aproximation, when (4.10) is substituted in (2.46), we must disregard $(\delta f)^2$ terms, and obtain

$$\begin{aligned} Z = \sum_{\{M_R\}} \exp[\pi K \sum_{R \neq R'} (M_R - f_o) G(R - R')(M_{R'} - f_o) \\ + 2\pi K f_o \sum_{R'} \int \frac{d^2 \vec{R}}{a^2} \ \vec{\nabla}_R \cdot \vec{u}_R \, G(R - R')(M_{R'} - f_o)] \end{aligned} \tag{4.11}$$

A partial integration in the last term finally gives

$$\begin{aligned} Z = \sum_{\{M_R\}} exp[\pi K \sum_{R \neq R'} (M_R - f_o) \ln \frac{|\vec{R} - \vec{R'}|}{a} (M_{R'} - f_o) + \ln y \sum_R (M_R - f_o)^2 \\ + 2\pi K f_o \sum_{R'} \int \frac{d^2 \vec{R}}{a^2} \ \vec{u}_R \cdot \frac{(\vec{R} - \vec{R'})}{|\vec{R} - \vec{R'}|^2} (M_{R'} - f_o)] \end{aligned} \tag{4.12}$$

where y is the vortex fugacity $y \simeq e^{-\pi^2 K/2}$ and the vortices satisfy the neutrality condition $\sum_R (M_R - f_o) = 0$.

A more careful derivation taking into account the differences between the original and dual lattices gives the same result to linear order in the displacements. Higher order terms in fact can be shown to make no difference to the final result.

This can be viewed as a coulomb gas of fractional charges perturbed by a random distribution of dipoles $\vec{p}_R \propto \vec{u}_R$. Here we concentrate only on the case where f_o is an integer. In this case shifting $M_R \rightarrow M_R + f_o$, we obtain a coulomb gas of integer charges perturbed by a random distribution of dipoles. This problem has been previously studied by Rubinstein et al (1983) in another context.

Renormalization-group recursion relations for this case can be conveniently constructed by the replica trick. Identical results can be obtained, although in a more laborious way, without using replicas. Proceeding with the replica trick (4.6), after performing the gaussian average in $\vec{u}_r$ using the distribution (4.5), we obtain from (4.12) the replicated coulomb gas Hamiltonian

$$\begin{aligned} -\frac{H}{k_B T} &= \pi K_1 \sum_{R \neq R'} \sum_{\alpha} M_R^{\alpha} M_{R'}^{\alpha} \ln \frac{|\vec{R} - \vec{R'}|}{a} \\ &\quad - \pi K_2 \sum_{R \neq R'} \sum_{\alpha \neq \beta} M_R^{\alpha} M_{R'}^{\beta} \ln \frac{|\vec{R} - \vec{R'}|}{a} \\ &\quad + \ln y \sum_{R} \sum_{\alpha} (M_R^{\alpha})^2 \end{aligned} \tag{4.13}$$

where

$$\begin{aligned} K_1 &= K - 4\pi^2 f_o^2 \Delta^2 K^2 \\ K_2 &= -4\pi^2 f_0^2 \Delta^2 K^2 \end{aligned} \tag{4.14}$$

Recursion relations for the above Hamiltonian can be obtained by the same procedure as described in Chapter 3. We obtain

$$\begin{aligned}
\frac{dK_1}{dl} &= -4\pi^3 y^2 [K_1^2 + (n-1)K_2^2] \\
\frac{dK_2}{dl} &= -4\pi^3 y^2 [2K_1 K_2 + (n-2)K_2^2] \\
\frac{dy}{dl} &= (2 - \pi K_1) y
\end{aligned} \tag{4.15}$$

Taking the limit $n \to 0$, we finally obtain

$$\begin{aligned}
\frac{dK_1}{dl} &= -4\pi^3 y^2 [K_1^2 - K_2^2] \\
\frac{dK_2}{dl} &= -4\pi^3 y^2 [2K_1 K_2 - 2K_2^2] \\
\frac{dy}{dl} &= (2 - \pi K_1) y
\end{aligned} \tag{4.16}$$

Combining the first two of the equations (4.16) and noting that $K_1 - K_2 = K$ gives

$$\begin{aligned}
\frac{dK}{dl} &= -4\pi^3 y^2 K^2 \\
\frac{dy}{dl} &= (2 - \pi K + 4\pi^3 f_o^2 \Delta^2 K^2) y
\end{aligned} \tag{4.17}$$

Note that f_o and Δ appear in the combination $f_o \Delta$ which can be regarded as a measure of the disorder which increases linearly with the applied field. For a given sample Δ is fixed and the degree of disorder is varied by changing f_o.

The renormalization group flows generated by equations (4.17) in the (K^{-1}, y) plane are shown in Figure 4.1 for small values of $f_o \Delta$.

There are two special points along the $y = 0$ line where the eigenvalue of y vanishes

$$K_{\pm}^{-1}(f_o \Delta) = \frac{\pi}{4}\left[1 \pm (1 - 32\pi f_o^2 \Delta^2)^{\frac{1}{2}}\right] \tag{4.18}$$

The heavy line in Figure 4.1 correspond to a trajectory which start at a special point K_o^{-1} below K_-^{-1} and ends at K_+^{-1}. The region bounded by this trajectory is a domain of atraction of the line $y = 0$. This correspond to the superconducting phase where thermal excited vortex pairs are bound in pairs and correlations decay algebraically. Below K_o^{-1}, the fugacity is relevant due to the random dipole potential. In the region $K_o^{-1} < K < K_+^{-1}$, there are enough vortex pairs to screen out this potential. As $f_o \Delta$ aproaches $\frac{1}{\sqrt{32\pi}}$, K_+^{-1} and

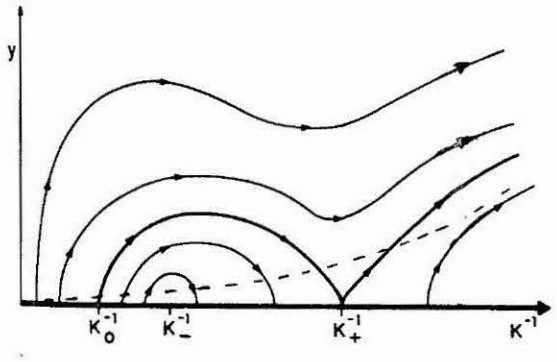

Figure 4.1 Renormalization-group flows. The heavy trajectory starting in K_o^{-1} and ending in K_+^{-1} bounds the superconducting region. The dotted line indicates a locus of initial conditions.

K_-^{-1} merge and the superconducting phase shrinks to zero. This leads to a critical value of f_o

$$f_M = \frac{1}{\sqrt{32\pi}} \frac{1}{\Delta} \tag{4.19}$$

above which there is no superconducting phase.

Figure 4.2 shows the resulting phase diagram. For sufficiently small f_o there is the usual resistive transition at a temperature $T_c = T^+(f_o)$. In contrast with the pure model one also finds a reentrant unbinding transition at a lower temperature $T^-(f_o)$. These temperatures are determined by the intersection of the curve of initial values (dotted line in Figure 4.1) with the phase boundary of the renormalization-group flows which separates the two regions where y is relevant and irrelevant.

The properties of both transitions are determined by the renormalization-group flows near K_+^{-1}. The exponent η characterizing the algebraic decay of the correlation function approaches the value

$$\eta^*(f_o\Delta) = \frac{1}{8}\left[1 + (1 - 32\pi\Delta^2 f_o^2)^{\frac{1}{2}}\right] + 2\pi\Delta^2 f_o^2 \tag{4.20}$$

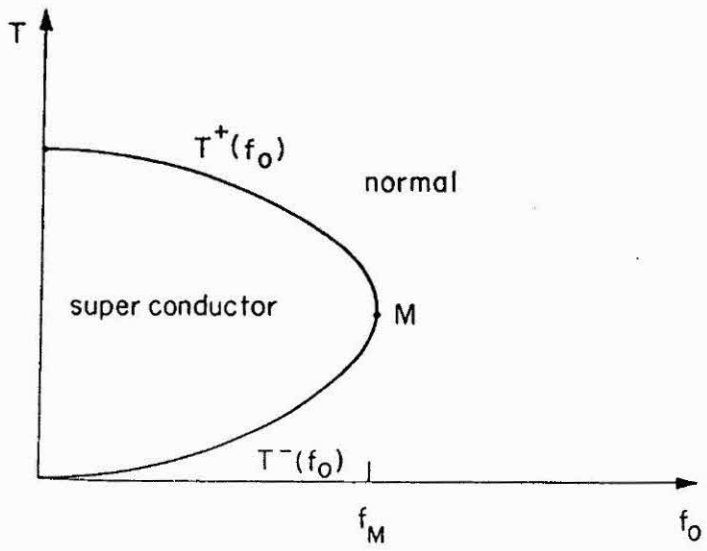

Figure 4.2 Qualitative phase diagram as a function of the temperature and average number of flux quanta per plaquette f_o. In the case we are considering here f_o is an integer.

at the two phase broundaries $T^{\pm}(\Delta f_o)$. In the normal phase, there is the usual exponential decay of the correlations. Near $T^{\pm}$, ξ diverge exponentialy like

$$\xi \sim \exp\left[C|T - T_o^{\pm}|^{-\frac{1}{2}}\right] \tag{4.21}$$

where C is a constant, for constant f_o. This result is the same of that obtained for the pure XY model (Equation 2.27). At constant temperature we obtain

$$\xi \sim \exp\left[C|f_o - f_c(T)|^{-\frac{1}{2}}\right] \tag{4.22}$$

The renormalized spin-wave stiffness constant approaches

$$K_R = \frac{1}{8\pi^2\Delta^2 f_o^2}\left[1 - (1 - 32\pi\Delta^2 f_o^2)^{\frac{1}{2}}\right] \tag{4.23}$$

on the phase boundaries of the superconducting phase. Therefore, in contrast with the pure system (Equation 2.26) the superfluid density jump is not universal but depends on f_o.

For $f_o \geq f_c$, the density of free vortices where $M_R = f_o \pm 1$ is approximatly $n_f \sim \xi^{-2}$ and so the resistance increases very slowly at constant temperature as f_o is increased beyond f_c. At higher fields, since the superconducting phase is unstable at any temperature, one

expects that this will cross-over to the usual flux-flow resistance discussed in Section 2.3.2, i.e., $R(H) \sim H$.

Chapter 5

RESISTANCE OSCILLATIONS IN THE IBM ARRAYS

5.1 Introduction

As we discussed in the previous Chapters, the simple model for an idealized superconducting array described in Section 2.2 can explain the main features of the experimental data in particular the basic periodicity in f and also the existence of subsidiary minima at rational values of f. However, there are certain features of the experimental results that have not been explained.

The frustrated XY model used predicts that the resistance minima at integer values of the flux should be zero at low temperatures (except for finite size effects) and should remain zero until the applied magnetic field reaches its critical value at which the superconducting elements making up the array go normal. The experiments, however, seem to disagree with this at least in two respects, except of course at zero field. First, the resistance minima never reaches zero except at zero field (Figures 1.1 - 1.2). Second, as can be seen in Figure 1.1, in the IBM arrays studied by Voss and Webb (1982) and Webb et al (1983) the resistance minima oscillate with a rather long period and beyond some critical value of the field these resitance minima start rising slowly and linearly at higher fields.

The first point has been considered in Section 4.2. In this Chapter we address the second point. We propose an interpretation of the variation of the resistance minima without disorder by modifying the simple model considered in Section 2.2 to include the presence of two incommensurate fundamental areas. The linear increase of the resistance at higher fields is then accounted for by including an small amount of positional disorder as described

in Chapter 4. In consequence, the fact that the critical field is also associated with the development of a minimum in the lower envelope of the resistance curve must be attributed to a coincidence since these two effects are independent of each other (Kosterlitz and Granato, 1986).

5.2 The model

The array studied by Voss and Webb (1982), consists of niobium superconducting wires in form of crosses and squares of $1\mu m$ cross section. The Nb tunnel junctions were patterned on oxidized Si chips. Whenever a cross overlaps a square a Josephson junction of $1\mu m^2$ of area is formed as laid out in Figure 5.1. We will assume the junction to be simultaneously large enough so that charging effects can be ignored but sufficiently small so that the field dependence of the effective coupling across the junction is negligible. In what follows, the finite size of the junction is completely ignored. We also make the further assumption that the superconducting elements are sufficiently thin so that flux can leak through them. With this assumption, the field is essentially uniform in the plane of the array and the system can be considered to be in thermal equilibrium. Note that a partial Meissner effect for the superconducting elements would lead to hysteresis and metastability and a total Meissner effect would completely eliminate the effect we are trying to explain.

We can immediately see that, under these physically reasonable assumptions, there is another area in the problem besides the fundamental area A_L formed by a loop containing four junctions. In the original analysis of Voss and Webb (1982), only the flux penetrating the area A_L was taken into account. This is responsible for the main oscillations with a period $\Delta B = \frac{\phi_o}{A_L} \sim .170e$. However, if this is the only area determining the period of the oscillations, the frustrated XY model defined in Section 2.2 would predict no further variation of the resistance which is contrary to the observation. With the assumption that flux can leak across the superconducting wires, there is another fundamental area A_s, the area of a square, which in general is incommensurate with A_L. Since the fast oscillations

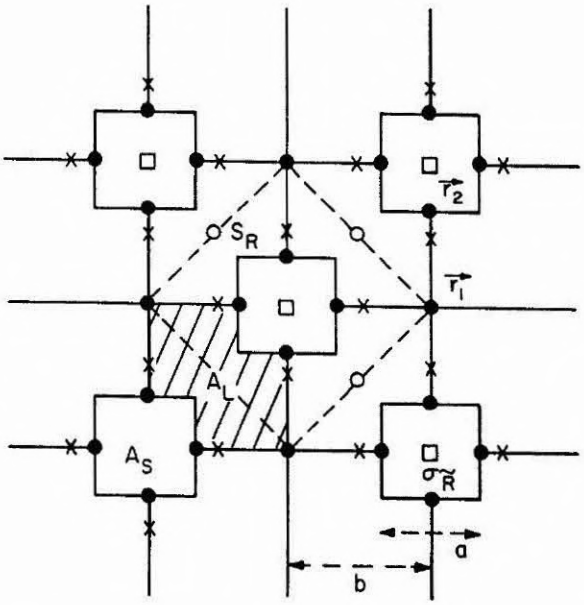

Figure 5.1 The IBM Josephson-junction array. Solid dots at $\vec{r}_1, \vec{r}_2$ represent the lattice of nodes of the superconducting network, crosses the weak links and solid lines the superconducting wires. The dual lattice sites are denoted by open dots (R) and squares ($\tilde{R}$). The two fundamental areas are the large squares (A_S) and hatched area (A_L). A unit cell is marked with a dashed line.

of the resistance are determined mainly by $f_L = \frac{BA_L}{\phi_o}$, we concentrate in particular on the minima at f_L = integer.

The Hamiltonian of the system can be parametrized as

$$\frac{H}{K_B T} = -K \sum_{<r_1 r_2>} \cos(\phi_{r_1} - \theta_{r_2} - A_{r_1 r_2}) - L \sum_{<r_2 r_2'>} \cos(\theta_{r_2} - \theta_{r_2'} - A_{r_2 r_2'}) \qquad (5.1)$$

where $A_{rr'} = \frac{2\pi}{\phi_o} \int_r^{r'} \vec{A} \cdot \vec{dl}$. In (5.1) two parameters K and L were introduced to describe the coupling across a junction between nodes on a cross and square (K) and between two nodes on a square (L), with $K << L$. Although the squares do not contain weak links, flux will leak in and out of the square so they have to be treated in the same way as the weak links but with a larger coupling constant. Of course the choice of the nodes of the network is completely arbitrary but a different choice makes no difference to the final result.

5.3 Coulomb gas representation

We can now follow the procedure of Section 2.4.2 in order to obtain the Coulomb gas Hamiltonian and write the partition function in the roughening representation. We obtain

$$Z = \Big[\prod_R \sum_{S_R}\Big]\Big[\prod_{\hat{R}} \sum_{\sigma_{\hat{R}}}\Big] \exp\Big[-\frac{1}{2K}\sum_{<RR'>}(S_R - S_{R'})^2 - \frac{1}{2L}\sum_{<R\hat{R}>}(S_R - \sigma_{\hat{R}})^2$$

$$- 2\pi f_L i\sum_R S_R - 2\pi f_S i\sum_{\hat{R}}\sigma_{\hat{R}}\Big] \tag{5.2}$$

where $f_S = Ba^2/\phi_o$ and $f_L = B(b^2 - \frac{a^2}{2})/\phi_o$ is the number of flux quanta through A_S and A_L respectively. The next step is to use the Poisson summation formula (2.45). This gives

$$Z = \Big[\prod_R \int_{-\infty}^{\infty} d\phi_R\Big]\Big[\prod_{\hat{R}} \int_{-\infty}^{\infty} \chi_{\hat{R}}\Big] \exp\Big[-\frac{1}{2K}\sum_{<RR'>}(\phi_R - \phi_{R'})^2 - \frac{1}{2L}\sum_{<R\hat{R}>}(\phi_R - \chi_{\hat{R}})^2$$

$$- 2\pi i\sum_R (f_L + M_R)\phi_R - 2\pi i\sum_{\hat{R}}(f_S + M_{\hat{R}})\chi_{\hat{R}}\Big] \tag{5.3}$$

To perform the resulting integration it is convenient to divide the dual lattice into unit cells with three charges per cell as shown in Figure 5.1. The resulting cells form a square lattice of lattice spacing $b\sqrt{2}$ with charges at the vertices and centers of the bonds. Splitting the ϕ_R variables into two interpenetrating square lattices, we can take Fourier transforms in which case we can write (5.3) as

$$Z = \Big[\prod_{i=1}^{3}\int d\phi_i(q)\Big] \exp\Big[-\frac{1}{2}\sum_q\sum_{i,j}\phi_i(q)G'^{-1}_{ij}(q)\phi_j(q)$$

$$- 2\pi i\sum_q\sum_i [M_i(q) + f_i(q)]\phi_i(q)\Big] \tag{5.4}$$

where i, j specify the intra-cell positions and $f_1 = f_2 = f_L$, $f_3 = f_S$. Here ϕ, χ have been

replace by ϕ_i and

$$G'^{-1}(q) = \begin{pmatrix} \frac{4}{K} + \frac{2}{L} & -\frac{2}{K}\left[\cos\frac{(q_x+q_y)}{2} + \cos\frac{(q_x-q_y)}{2}\right] & -\frac{2}{L}\cos\frac{1}{2}q_x \\ -\frac{2}{K}\left[\cos\frac{(q_x+q_y)}{2} + \cos\frac{(q_x-q_y)}{2}\right] & \frac{4}{K} + \frac{2}{L} & -\frac{2}{L}\cos\frac{1}{2}q_y \\ -\frac{2}{L}\cos\frac{1}{2}q_x & -\frac{2}{L}\cos\frac{1}{2}q_y & \frac{4}{L} \end{pmatrix} \tag{5.5}$$

Finally, performing the gaussian integrals we obtain the Coulomb gas Hamiltonian

$$\frac{H_c}{k_B T} = 2\pi^2 \sum_{i,j=1}^{3} \sum_{q} [M_i(q) + f_i(q)] G'_{ij}(q) [M_j(q) + f_j(q)] \tag{5.6}$$

We find $G'^{-1}_{ij}(0) = 0$ in which case $G'_{ij}(R)$ diverges logarithmically with the size of the system. However, taking the small q limit we find

$$G'_{ij}(q) = \frac{2LK}{2L+K}\left[\frac{1}{q^2}\delta_{ij} + E_{ij}\right] + O(q^2) \tag{5.7}$$

When $L >> K$, we obtain

$$E = E_o I + \begin{pmatrix} \frac{3K}{32} & -\frac{K}{32} & -\frac{K}{32} \\ -\frac{K}{32} & +\frac{3K}{32} & -\frac{K}{32} \\ -\frac{K}{32} & -\frac{K}{32} & +\frac{L}{4} \end{pmatrix} \tag{5.8}$$

where E_o is the usual core energy of a single vortex and I is the identity matrix. When (5.7) is substituted in (5.6) we obtain

$$\begin{aligned} \frac{H_c}{k_B T} = &-\frac{2\pi LK}{2L+K} \sum_{i,j} \sum_{R \neq R'} [M_i(R) + f_i][M_j(R') + f_j] \ln\left|\frac{(R-R')}{r_o}\right| \\ &+ \sum_{R} \sum_{i,j} [M_i(R) + f_i] E_{ij} [M_j(R) + f_j] \end{aligned} \tag{5.9}$$

The calculation of E_{ij} which is the short range part of the interaction G'_{ij} is an important step. If E_{ij} was neglected in (5.7), from (5.6) we could replace $\sum_i (M_i + f_i)$ by $\sum_i (M + f)$ where $f = 2f_L + f_S$ which is the number of flux quanta in one cell. This would make the

Coulomb gas Hamiltonian periodic in f which in turn implies a single periodicity of the resistance on the magnetic flux. Since the eigenvalue of E_{ij} are all positive and distinct, the energy minima occur when each f_i is equal to an integer, so the expected periodicity is restored by this short-range part.

5.4 Effects of competing areas and disorder

We can draw a few conclusions from the form of the Hamiltonian (5.9). If f_L and f_S are both integers, the system reduces to three coupled Coulomb gases with integer charges which can be studied by the methods of Chapter 3. In this case an XY-like transition is expected at a temperature determined by

$$\frac{\pi LK}{(2L+K)} \simeq 1 \tag{5.10}$$

This corresponds to the same behavior at zero field. At other values of f_L and f_S, the resistance will be controlled mainly by f_L and will be roughly proportional to $|f_L - n|$ where n is the closest integer to f_L (see Section 2.52). So we expect that the resistance can be approximated by

$$R(f_L, f_S) = A|f_L - n_L| + B|f_S - n_S| \tag{5.11}$$

where $A > B$ are proportional to the mobilities of the defects in the flux lattice.

Using the measured ratio of the areas $A_L/A_S \simeq 1.235$, we have $f_S = f_L A_S/A_L \simeq 0.809 f_L$ so the deviation δf_S of f_S from an integer will be minimum at certain values of f_L where f_L is restricted to an integer value. For this ratio of areas, these occur at $f_L = 0 (\delta f_S = 0)$, $f_L = 5, 16 (\delta f_S \simeq .05)$, $f_L = 10, 11 (\delta f_S \simeq .09)$ and $f_L = 21 (\delta f_S \simeq .004)$, etc. Thus from (5.11) we expect subsidiary minima in the lower envelope of the resistance curve at these values of f_L with the deepest one at $f_L = 21$, the next deepest at $f_L = 5, 16$ and the highest at $f_L = 10, 11$. Of course, since the areas are probably incommensurate, the resistance variations are only quasiperiodic and are rather sensitive to the exact value of the ratio.

When the magnetic field is increased further, randomness in the positions of the nodes of the superconducting array measured by a standard deviation Δ will disorder the su-

perconducting phase at some critical value dependent on Δ. Combining these two results together yields a lower envelope of the resistance which is in good qualitative agreement but a detailed comparison requires a much more sophisticated theory. The experimental observation by Webb et al (1983) that the deep minimum in resistance at $f_L \simeq 21 - 25$ (see Figure 1.1) is correlated with the beginning of the monotonic rise of the lower enevelope must be attributed to coincidence since the critical field and the exact value of f_L at the minimum are both sample dependent and independent of each other.

Appendix A

DOMAIN WALL ENERGY FOR THE FULLY FRUSTRATED XY MODEL

The coulomb gas energy for this case can be written as

$$E = -\sum_{R \neq R'} q_R \, q_{R'} \ln \frac{|\vec{R} - \vec{R'}|}{a} \qquad (A.1)$$

where $q_R = \pm q$ and $q = -\frac{\sqrt{2\pi J}}{2}$. The charges q_R are arranged in a chessboard ground state as in Figure 2.14.

Consider a single vertical domain wall in this ground state. It divides the system in two regions where one region, say (2), is obtained from region (1) by changing the sign of q_R. The domain wall energy is the excess energy produced by this configuration. It can easily be seen that this energy is given by $E_w = -2E_{(1),(2)}$ where $E_{(1),(2)}$ is the interaction energy between the lines of charges in one region with the other region. Since each line consists of alternating + and − charges, this is a very simple eletrostatic problem. The energy between two lines of charges separated by a distance R is given by

$$\frac{dE}{dR^2} = \pm q^2 \sum_{-\infty}^{\infty} \frac{(-1)^n}{R^2 + na^2} \qquad (A.2)$$

The series in the right hand side can be easily summed using complex integration and gives $-\frac{\pi a}{R}(\sinh \frac{\pi R}{a})^{-1}$. Substituting in (A1) we obtain

$$E_{int} = \pm q^2 \ln \tanh \frac{\pi R}{2a} \qquad (A.3)$$

where the + and − signs correspond to unequal and equal lines. For $R >> a$ this gives a exponential decay as in Equation (2.65).

The domain wall energy can now be obtained by adding up the interaction energy of the lines of charges of region (1) with those of region (2), i.e.

$$E_w = 2q^2 \sum_{P=1}^{\infty} \sum_{R=P}^{\infty} (-1)^{\frac{R}{a}} \ln \tanh \frac{\pi R}{2a} \qquad (A.4)$$

After using the approximation for large distances, this series can be summed to give

$$E_w = \frac{4e^{-\pi}}{(1+e^{-\pi})^2} q^2 = 0.27J \qquad (A.5)$$

Halsey (1985b) working with the original model (2.5) has obtained, using numerical methods, $E_w = 0.34J$. The small discrepancy is due to the fact that the transformation of the original Hamiltonian (2.5) into the coulomb gas representation (A.1) is not an exact one.

Appendix B

COULOMB GAS REPRESENTATION

Kadanoff (1978) has given a general prescription for transforming two-dimensional statistical mechanical models into a coulomb gas representation. In this Appendix we briefly outline the derivation.

The first step is the replacement of all cosine interaction terms by the Villain's approximation

$$e^{K\cos x} = \sum_{m=-\infty}^{\infty} e^{-\frac{K}{2}(x-2\pi m)^2} \qquad (B.1)$$

Using the Poisson summation formula (2.45) and performing the resulting gaussian integral the above expression can also be written as

$$e^{K\cos x} = \sum_{m=-\infty}^{\infty} e^{-\frac{1}{2K}m^2+imx} \qquad (B.2)$$

So the Villain's approximation consists basically in the replacement of the Fourier coefficients of $e^{K\cos x}$ by $I_m(K) \sim e^{-\frac{1}{2K}m^2}$ which is a good approximation for low temperatures. This is the same approximation we use in Section 2.4.2. Note that (B.1) has the same symmetry as the original cosine interaction. The difference between the Villain and cosine interactions was shown to be irrelevant to the critical behavior of the XY model (José et al, 1977). The Villain's approximation allow an exact decomposition of spin wave and vortex configurations as obtained in Equation (2.46).

Using this approximation, the partition function for the model (3.1) can be written as

$$Z = \Big[\prod_{<rr'>}\sum_{m_{rr'}}\sum_{n_{rr'}}\Big]\Big[\prod_{r}\sum_{S_r}\Big]\exp\Big[-\frac{\alpha}{2}\sum_{<rr'>}(\theta_r-\theta_{r'}-2\pi m_{rr'})^2$$
$$-\frac{\beta}{2}\sum_{<rr'>}(\phi_r-\phi_{r'}-2\pi n_{rr'})^2$$
$$-g\sum_{<rr'>}(\theta_r-\theta_{r'}-2\pi m_{rr'})(\phi_r-\phi_{r'}-2\pi n_{rr'})$$
$$+ip\sum_{r}S_r(\theta_r-\phi_r)+\ln y_0 S_r^2\Big] \qquad (B.3)$$

We now make use of the gauge-invariance of (B.3), i.e., the invariance of the integrand under a transformation

$$\theta_r \to \theta_r + 2\pi q_r$$
$$m_{rr'} \to m_{rr'} + q_r - q_{r'} \qquad (B.4)$$

where q_r is an integer. Similar transformations can be applied to the $n_{rr'}$ variables. Because of this invariance we can choose q_r and p_r such that on horizontal bonds $q_r - q_{r'} + m_{rr'} = 0$ and $p_r - p_{r'} + n_{rr'} = 0$. The remaining q_r and p_r appear in the combination $\theta_r + 2\pi q_r$ and $\phi_r + 2\pi p_r$ and can be used to extend the range of integrations of θ and ϕ from $-\infty$ to ∞.

The exponent in (B.3) is now reduced to

$$A = -\frac{\alpha}{2}\sum_{<rr'>}(\theta_r-\theta_{r'})^2-\frac{\beta}{2}\sum_{<rr'>}(\phi_r-\phi_{r'})^2-g\sum_{<rr'>}(\theta_r-\theta_{r'})(\phi_r-\phi_{r'})$$
$$+2\pi\sum_{<rr'>}^{|}(\theta_r-\theta_{r'})(\alpha m_{rr'}-\beta n_{rr'})+2\pi\sum_{<rr'>}^{|}(\phi_r-\phi_{r'})(\alpha n_{rr'}-\beta m_{rr'})$$
$$ip\sum_{r}S_r(\theta_r-\phi_r) \qquad (B.5)$$

Here, $\sum_{<rr'>}^{|}$ denotes the sum over vertical bonds only.

Each quadratic form in (B.5) can be written as

$$\sum_{<rr'>}(\theta_r-\theta_{r'})^2=\sum_{r,r'}\theta_r G^{-1}_{rr'}\theta_{r'} \qquad (B.6)$$

where $G_{rr'}$ is the lattice Green's function. It diverges at $r = r'$ (see for example José et al, 1977). To isolate the divergence $G_{rr'}$ can be splitted in two parts

$$G_{rr'} = -\frac{1}{2\pi}G(r-r') + G(0) \qquad (B.7)$$

with a large distance behavior $G(r-r') \sim \ln \frac{|\vec{r}-\vec{r}'|}{a} + \frac{\pi}{2}$, and $G(0) \to \infty$.

After performing the gaussian integrations in (B.4) and using (B.5), the resulting expression in terms of $m_{rr'}$ and $n_{rr'}$ can be simplified if new variables in the dual lattice are defined by

$$M_R = \sum_R m_{rr'}, \qquad N_R = \sum_R n_{rr'} \tag{B.8}$$

where $\sum_R$ means a discrete curl around a plaquette with dual site $\vec{R}$. The detailed calculation that follows can be found in Kadanoff (1978) and also in the Appendix of the paper by Yosefin and Domany (1985). The singular term $G(0)$ imposes charge neutrality conditions

$$\sum_R M_R = \sum_R N_R = \sum_r S_r = 0 \tag{B.9}$$

With these definitions, one obtain the representation (3.8). The same procedure can be applied to obtain coulomb gas representations for the correlation functions.

Kadanoff's method, although systematic and straighforward, is sometimes unecessary for the kinds of models studied in Chapter 3. As noted by Nelson and Halperin (1980), the final result can be easily obtained by expanding from the beginning θ_r and ϕ_r about vortex configurations as

$$\begin{aligned} \theta_r &= \theta_r^o + \sum_R M_R \Theta(r-R) \\ \phi_r &= \phi_r^o + \sum_R N_R \Theta(r-R) \end{aligned} \tag{B.10}$$

where $\Theta(r-R)$ has the assymptotic form given in (3.11) and θ_r^o, ϕ_r^o are smooth functions which correspond to the spin wave part. This is the same expansion used originally by Kosterlitz (1974) to obtain the coulomb gas Hamiltonian for a single XY model. Since (B.10) contains vortices explicitly, the action can be simply approximated by a gaussian

$$\begin{aligned} A = &-\frac{\alpha}{2}\int d^2 r(\nabla\theta)^2 - \frac{\beta}{2}\int d^2 r(\nabla\phi)^2 - g\int d^2 r \nabla\theta\cdot\nabla\phi \\ &+ ip\sum_r S_r(\theta_r - \phi_r) \end{aligned} \tag{B.11}$$

The quadratic terms have been temporarily approximated by their continuum forms for convenience of calculation. Inserting the expansions (B.10) and noting that spin wave and

vortices decouple in this approximation, we obtain after performing the required gaussian integrals

$$
\begin{aligned}
A = & -\frac{\alpha}{2}\sum_{R,R'} M_R M_{R'} \int d^2 r \nabla\Theta(r-R)\nabla\Theta(r-R') \\
& -\frac{\beta}{2}\sum_{R,R'} N_R N_{R'} \int d^2 r \nabla\Theta(r-R)\nabla\Theta(r-R') \\
& -g\sum_{R,R'} M_R N_{R'} \int d^2 r \nabla\Theta(r-R)\nabla\Theta(r-R') \\
& -\frac{p^2}{2(\alpha\beta-g^2)}(\alpha+\beta+2g)\sum_{r,r'} S_r G_{rr'} S_{r'}
\end{aligned}
\qquad (B.12)
$$

Using the large distance behavior $G_{rr'} = -\frac{1}{2\pi}\ln\frac{|\vec{r}-\vec{r}'|}{a}$ and regarding $G_{rr'}$ as a function of complex variable we have the property $\Theta(r-r') = -2\pi\, Im G_{rr'}$. Using the Cauchy-Rienman relations for complex functions, integrating by parts and using the property $\nabla^2 G_{rr'} = -\delta_{rr'}$, the integrals in the first three terms of (B.12) can be performed to give

$$
\int d^2 r \nabla\Theta(r-R)\nabla\Theta(r-R') = (2\pi)^2 G_{RR'} \qquad (B.13)
$$

Using (B.13) we obtain directly (3.8). The same procedure can be easily applied to the correlation functions (Equations 3.12 - 3.16).

Appendix C

RECURSION RELATIONS IN THE COULOMB GAS REPRESENTATION

In this Appendix we outline a derivation of the renormalization-group recursion relations for the kind of Coulomb gas Hamiltonians studied in Chapter 3. Further details can be found in Kosterlitz (1974) and Nelson and Halperin (1980). We also include in this Appendix a derivation of recursion relations in the presence of hybrid vortices.

Consider a simpler case with only M_R and S_r vortices. Setting $M_R = 0$ in (3.8) and restricting attention only to excitations with charge ± 1, we expand the partition function as power series in each fugacity as

$$Z = \sum_{N=0}^{\infty} \sum_{N'=0}^{\infty} \frac{1}{N!^2} \frac{1}{N'!^2} \left[\frac{y_m}{a^2}\right]^{2N} \left[\frac{y_s}{a^2}\right]^{2N'} \left[\prod_{i=1}^{2N} \int d^2 R_i\right] \left[\prod_{j=1}^{2N'} \int d^2 r_j\right] e^{A_{N,N'}} \qquad (C.1)$$

where N and N' are the number of the M and S charge pairs respectively, and

$$A_{N,N'} = \pi\alpha \sum_{i \neq j} M_{R_i} M_{R_j} G(R_i - R_j) + ip \sum_{i \neq j} S_{r_i} M_{R_j} \Theta(r_i - R_j) + \pi\gamma \sum_{i \neq j} S_{r_i} S_{r_j} G(r_i - r_j) \quad (C.2)$$

To take into account the underlying lattice each integration in (C.1) is excluded from circles of radius a centered at the positions $\vec{r}_i$ and $\vec{R}_i$ of the others charges. In order to contruct the renormalization transformation we scale the minimum charge separation from a to ae^{δ} and explicitly integrate out those configurations where two opposite charge approach each other with separations between a and ae^{δ} with δ small. Recursion relations for the parameters can then be obtained by finding the correction to the partition function resulting from this procedure and requiring for the new partition function the same functional form as the original one.

To linear order in δ we can rearrange the integrand in (C.1) as

$$\left[\prod_{i=1}^{2N}\int d^2R_i\right]\left[\prod_{j=1}^{2N'}\int d^2r_j\right] = \left[\prod_{i=1}^{2N}\int^{>} d^2R_i\right]\left[\prod_{j=1}^{2N'}\int^{>} d^2r_j\right]$$

$$+\frac{1}{2}\sum_{k\neq l}\left[\prod_{\substack{i=1\\ i\neq k,l}}^{2N}\int^{>} d^2R_i\right]\left[\prod_{j=1}^{2N'}\int^{>} d^2r_j\right]\int d^2R_k\int_{\delta(k)} d^2R_l$$

$$+\frac{1}{2}\sum_{t\neq u}\left[\prod_{i=1}^{2N}\int^{>} d^2R_i\right]\left[\prod_{\substack{j=1\\ j\neq t,u}}^{2N'}\int^{>} d^2r_j\right]\int d^2r_t\int_{\delta(t)} d^2r_u$$

$$+O(\delta^2) \qquad (C.3)$$

where the integral $\int^{>}$ exclude circles of radii ae^{δ} centered at all others charges. The integral over $\delta(k)$ indicates an integration over the annulus $a < |\vec{R}_k - \vec{R}_l| < ae^{\delta}$ centered at the charge at site $\vec{R}_k$. The sum in the second term of (C.3) takes into account only pairs of charges of the same kind. Consideration of pairs of different charges correspond to the inclusion of hybrid vortices. These can be considered as composite vortices and should be included from the begining. For the same reason, we consider only pairs of opposite charges.

After these considerations, the next step is to carry out explicitly the integration over R_k, R_l, r_t and r_u in (C.3). Consider the terms in $A_{N,N'}$ which depends on R_k, R_l and r_t, r_u

$$I_{kl} = \int d^2R_k\int_{\delta(k)} d^2R_l\exp\left[2\pi\alpha\sum_{\substack{i=1\\ i\neq k,l}}^{N} M_{R_i}[G(R_i-R_k)-G(R_i-R_l)]\right.$$
$$\left.+ip\sum_{\substack{i=1\\ i\neq k,l}}^{N'} S_{r_i}[\Theta(r_i-R_k)-\Theta(r_i-R_l)]\right] \qquad (C.4)$$

and

$$I_{tu} = \int d^2r_t\int_{\delta(t)} d^2r_u\exp\left[2\pi\gamma\sum_{\substack{i=1\\ i\neq t,u}}^{N'} S_{r_i}[G(r_i-r_t)-G(r_i-r_u)]\right.$$
$$\left.+ip\sum_{\substack{i=1\\ i\neq t,u}}^{N} M_{R_i}[\Theta(r_t-R_i)-\Theta(r_u-R_i)]\right] \qquad (C.5)$$

It is convenient to change variables in the integrations in (C.4) and (C.5) as

$$\begin{aligned} \vec{x} &= \vec{r}_t - \vec{r}_u, \qquad \vec{y} = \frac{1}{2}(\vec{r}_t + \vec{r}_u) \\ \vec{X} &= \vec{R}_k - \vec{R}_l, \qquad \vec{Y} = \frac{1}{2}(\vec{R}_k + \vec{R}_l) \end{aligned} \tag{C.6}$$

Expanding the exponential in (C.4) and (C.5) to second order in $\vec{y}$ and $\vec{Y}$ we obtain

$$I_{kl} = \int d^2x \int d^2y \Big[1 + (2\pi\alpha)^2 \sum_{i,j} M_{R_i} M_{R_j} [\vec{Y} \cdot \nabla_X G(R_i - X)][\vec{Y} \cdot \nabla_X G(R_j - X)]$$

$$- p^2 \sum_{i,j} S_{r_i} S_{r_j} [\vec{Y} \cdot \nabla_X \Theta(r_i - X)][\vec{Y} \cdot \nabla_X \Theta(r_j - X)] \Big] \tag{C.7}$$

and similarly for I_{tu} in (C.5). Note that the first order term in y or Y and the cross-term of the form $\nabla\Theta\nabla G$ are identically zero when the integration is performed. Averaging over the orientations of $\vec{Y}$, using the property of the harmonic conjugates, i.e., $(\nabla G)^2 = (\nabla\Theta)^2$ and using (B.15) we obtain from (C.7)

$$I_{kl} = 2\pi a^2 \delta \Big[A - (2\pi\alpha)^2 \pi a^2 \sum_{i,j} M_{R_i} M_{R_j} G(R_i - R_j) + p^2 \pi a^2 \sum_{i,j} S_{r_i} S_{r_j} G(r_i - r_j) \Big] \tag{C.8}$$

Similarly

$$I_{tu} = 2\pi a^2 \delta \Big[A - (2\pi\gamma)^2 \pi a^2 \sum_{i,j} S_{r_i} S_{r_j} G(r_i - r_j) + p^2 \pi a^2 \sum_{i,j} M_{R_i} M_{R_j} G(R_i - R_j) \Big] \tag{C.9}$$

Using (C.3), (C.8) and (C.9) and rearranging the summation in the additional term, we can write the partition function as

$$Z = \sum_{N=0}^{\infty} \sum_{N'=0}^{\infty} \frac{1}{N!^2} \frac{1}{N'!^2} \left[\frac{y_m}{a^2} \right]^{2N} \left[\frac{y_e}{a^2} \right]^{2N'} \left[\prod_{i=1}^{2N} \int d^2 R_i \right] \left[\prod_{j=1}^{2N'} \int d^2 r_j \right] e^{A_{N,N'}}$$

$$\times \Big[1 + \frac{y_m^2}{(N+1)^2} \sum_{k,l=1}^{N+1} 2\pi\delta \Big[\frac{A}{a^2} - 4\pi^3\alpha^2 \sum_{i,j} M_{R_i} M_{R_j} G(R_i - R_j)$$

$$+ \pi p^2 \sum_{i,j} S_{r_i} G(r_i - r_j) S_{r_j} \Big]$$

$$+ \frac{y_e^2}{(N'+1)^2} \sum_{t,u=1}^{N'+1} 2\pi\delta \Big[\frac{A}{a^2} - 4\pi^3\gamma^2 \sum_{i,j} S_{r_i} S_{r_j} G(r_i - r_j)$$

$$+ \pi p^2 \sum_{i,j} M_{R_i} M_{R_j} G(R_i - R_j) \Big] \Big] \tag{C.10}$$

The $(N+1)^2$ and $(N'+1)^2$ denominators are cancelled by the double summations. Since the additional term is of order δ, we can take the exponential to obtain an action of the same form as (C.2), but with coupling parameters replaced by

$$\begin{aligned} \alpha &\to \alpha - 4\pi^3 \alpha^2 y_m^2 + \pi p^2 y_e^2 \\ \gamma &\to \gamma - 4\pi^3 \gamma^2 y_e^2 + \pi p^2 y_m^2 \end{aligned} \tag{C.11}$$

Finally, we change $a \to a + a\delta$ in the new partition function to bring the resulting expression in the same form as the original one except that now the cut-off distance has been increased from a to ae^{δ}. It can easily be seen that this only changes the fugacity since

$$\pi\alpha \sum_{i,j} M_{R_i} M_{R_j} \ln \frac{\vec{R}_i - \vec{R}_j}{a} \to \pi\alpha \sum_{i,j} M_{R_i} M_{R_j} \ln \frac{\vec{R}_i - \vec{R}_j}{ae^{\delta}} - \pi\alpha\delta \sum_i M_{R_i}^2 \tag{C.12}$$

From (C.11) and (C.12) we find renormalized couplings $\alpha(l), \gamma(l)$ and $y(l)$, where the lattice spacing has been increased from a to ae^l, given by the equations

$$\begin{aligned} \frac{dy_m}{dl} &= (2 - \pi\alpha) y_m \\ \frac{dy_e}{dl} &= (2 - \pi\gamma) y_e \\ \frac{d\alpha}{dl} &= -4\pi^3 \alpha^2 y_m^2 + \pi p^2 y_e^2 \\ \frac{d\gamma}{dl} &= -4\pi^3 \gamma^2 y_e^2 + \pi p^2 y_m^2 \end{aligned} \tag{C.13}$$

The procedure can be easily generalized for the more general case of the Actions (3.8) or (3.46).

Now consider recursion relations for (3.8) when hybrid vortices are also included. Only hybrid vortices in which an M vortex and an N vortex have the same sign are found to be relevant when $g < 0$. If we regard these hybrid vortices as composite vortices we can

rewrite the Action (3.8) as

$$A = \pi\alpha \sum_{R,R'} M_R\, G(R - R')M_{R'} + \pi\beta \sum_{R,R'} N_R\, G(R - R')N_{R'}$$

$$+ 2\pi g \sum_{R,R'} M_R\, G(R - R')N_{R'} + ip \sum_{r} \sum_{R} S_r\, \Theta(r - R)M_R$$

$$- ip \sum_{r} \sum_{R} S_r\, \Theta(r - R)N_R + \pi\gamma \sum_{r,r'} S_r\, G(r - r')S_{r'}$$

$$+ 2\pi(\alpha + g) \sum_{R,R'} M_R\, G(R - R')H_{R'} + 2\pi(\beta + g) \sum_{R,R'} N_R\, G(R - R')H_{R'}$$

$$+ \pi(\alpha + \beta + 2g) \sum_{R,R'} H_R\, G(R - R')H_{R'} \qquad (C.14)$$

Where H_R is a hybrid vortex at site $\vec{R}$ and the summation over M_R and N_R exclude positions where they reside at the same site. Recursion relations can now be obtained by the same procedure as described before. We obtain

$$\begin{aligned}
\frac{dy_m}{dl} &= (2 - \pi\alpha)y_m \\
\frac{dy_n}{dl} &= (2 - \pi\beta)y_n \\
\frac{dy_s}{dl} &= (2 - \pi\gamma)y_s \\
\frac{dy_H}{dl} &= [2 - \pi(\alpha + \beta + 2g)]y_H \qquad (C.15) \\
\frac{d\alpha}{dl} &= -4\pi^3\alpha^2 y_m^2 - 4\pi^3 g^2 y_n^2 + \pi p^2 y_s^2 - 4\pi^3(\alpha + g)^2 y_H^2 \\
\frac{dg}{dl} &= -4\pi^3\alpha g y_m^2 - 4\pi^3\beta g y_n^2 - \pi p^2 y_s^2 - 4\pi^3(\alpha + g)(\beta + g)y_H^2 \\
\frac{d\beta}{dl} &= -4\pi^3\beta^2 y_n^2 - 4\pi^3 g^2 y_m^2 + \pi p^2 y_s^2 - 4\pi^3(\beta + g)^2 y_H^2
\end{aligned}$$

We note that the initial relation (3.9) and the initial form of the couplings $\alpha + \beta, \beta + g$ and $\alpha + \beta + 2g$ in (C.14) are all preserved under renormalization.

From the recursion relations for the y_H fugacity we find that the y_H is irrelevant for $\pi\alpha + \pi\beta > 2$ when $g = 0$ initially. However as $g < 0$, hybrid vortices are relevant in the region where the XY and the Ising lines of Figure (3.1) meet.

For the Action (3.34), the relevant hybrid vortices are the ones made up of K and L vortices of opposite signs. In this case we obtain the recursion relations

$$\begin{aligned}
\frac{dy_K}{dl} &= (2 - \pi\alpha_2)y_K \\
\frac{dy_L}{dl} &= (2 - \pi\beta_2)y_L \\
\frac{dy_s}{dl} &= (2 - \pi\gamma_2)y_s \\
\frac{dy_H}{dl} &= [2 - \pi(\alpha_2 + \beta_2 - 2g)]y_H \\
\frac{d\alpha_2}{dl} &= -4\pi^3\alpha_2^2 y_K^2 - 4\pi^3 g_2^2 y_L^2 + 4\pi^3(\alpha_2 - g_2)^2 y_H^2 \\
\frac{dg_2}{dl} &= -4\pi^3\alpha_2 g_2 y_K^2 - 4\pi^3\beta_2 g_2 y_L^2 + 4\pi^3(\alpha_2 - g_2)(\beta_2 - g_2)y_H^2 \\
\frac{d\beta_2}{dl} &= -4\pi^3\beta_2^2 y_L^2 - 4\pi^3 g_2^2 y_K^2 + \pi p^2 y_s^2 - 4\pi^3(\beta_2 - g_2)^2 y_H^2
\end{aligned} \tag{C.16}$$

If we now write α_2, g_2 and β_2 in terms of the initial values, i.e., $\alpha_2 = \alpha + \beta + 2g$, $\beta_2 = \beta$ and $g_2 = -\beta - g$, when this relations are substituted in (C.16) we obtain the same recursions as in (C.15) provided we identify the vortices as $K \to H, H \to M$ and $L \to N$.

REFERENCES

Beasley M R, Mooij J E and Orlando T P 1979, Phys. Rev. Lett. **42** 1165

Berenzinskii V L 1970, Zh. Eksp. Teor. Fiz. **59**, 907

Berge B, Diep H T, Ghazali A and Lallemand P 1986, to appear in J Phys C

Bishop D J and Reppy J D 1978, Phys. Rev. Lett. **40** 1727

Choi M Y and Doniach S 1985, Phys Rev B **31** 4516

Chui S T and Weeks J D 1976, Phys. Rev. B **14**, 4978

Claro F. H. and Wannier G. H. 1979, Phys. Rev. B **19**, 6068

Davidson A and Tsuei C C 1981, Physica **108**B, 1243

Edwards S F and Anderson P W 1975, J. Phys. F **5**, 965

Einhorn M B, Savit R and Rabinovic E 1980, Nucl. Phys. B **170**, 16

Elitzur A, Pearson R B and Shigemitsu J 1979, Phys. Rev. D **19**, 3698

Fradkin E, Huberman B A and Shenker S H 1978, Phys. Rev. B **18**, 4789

Garel T and Doniach S 1980, J. Phys. C **13**, L887

Goldman A M and Wolf S A 1984 (eds), *Percolation, Localization and Superconductivity*, Plenum Press, N.Y.

Granato E and Kosterlitz J M 1986a, Phys. Rev. B **33**, 4767

Granato E and Kosterlitz J M 1986b, J. Phys. C **19**, L59

Granato E and Kosterlitz J M 1986c, Phys. Rev. B **33** (to appear)

Gubser D U, Francavilla T L, Leibowitz J R and Wolf S A 1980, *Inhomogeneous Superconductors*, American Institute of Physics

Halsey T 1985a, Phys. Rev. B **31**, 5728

Halsey T 1985b, J. Phys. C **18**, 2437

Heinekamp S W and Pelcovits R A 1985, Phys. Rev. B **32** 4528

Hertz J A 1978, Phys. Rev. B **18**, 4875

Hofstadter D R 1976, Phys. Rev. B **14**,2239

Hubbard J 1959, Phys. Rev. Lett. **3**, 77

José J V, Kadanoff L P, Kirpatrick S and Nelson D R 1977, Phys Rev B **16** 1217

José J V 1984, Phys. Rev. B **29**, 2836

Kadanoff L P 1976, Ann. Phys. (N Y) **100**, 359

Kadanoff L P 1978, J. Phys. A **11**, 1399

Kimhi D, Leyraz and Ariosa D 1984, Phys. Rev. B **29**,1487

Kogut J B 1979, Rev. Mod. Phys. **51**, 659

Kosterlitz J M and Thouless D J 1973, J. Phys. C **6**, 1181

Kosterlitz J M and Thouless D J 1978, Prog. Low Temp. Phys. **78**, 551

Kosterlitz J M 1974, J. Phys. C **7**, 1046

Kosterlitz J M and Granato E 1986, submitted for publication

Lee D H, Joannopolos, Negele J W and Landau D P 1986, Phys. Rev. B **33**, 450

Lee D H and Grinstein G 1985, Phys. Rev. Lett. **55**, 541

Lobb C J, Abraham D W and Tinkham M 1983, Phys. Rev. B **27** ,150

Migdal A A 1975, Zh. Eksp. Teor. Fiz. **69**, 1457

Miyashita S and Shiba H 1984, J. Phys. Soc. Jpn **53**, 1145

Mukamel D 1975, Phys. Rev. Lett. **34**, 481

Nelson D R 1983, in *Phase transitions and Critical Phenomena* , C D Domb and J R Lebowitz (eds), Academic Press London

Nelson and Halperin 1980, Phys. Rev. B **21**, 5312

Pannetier B, Claussy J and Rammal R 1983, J. Phys. (Paris) Lett. **44**, L853

Parga N and Himbergen J E, Solid State Commun. **35**, 607

Pearl J 1965, in *Low Temperature Physics-LT9*, J G Daunt, D O Edwards, F J Milford and M Yaqub (eds), Plenum Press, N.Y.

Rammal R, Lubensky T C and Toulouse 1983, Phys. Rev. B **27**, 2820

Resnick D J, Brown R K, Rudman D A and Garland J C 1984, in *Low Temperature Physics-LT9*, U Eckern, A Schmid, W Weber and H Wuhl (eds), Elsevier Publishers

Ritala R A 1984, J. Phys. C **17**, 449

Rubinstein M, Shraiman B and Nelson D R 1983, Phys. Rev. B **27**, 1800

Shih W Y and Stroud D 1985, Phys. Rev. B **32**, 158

Stratonovich R L 1957, Dokl. Akad. Nauk. SSSR **115**, 1097

Swendsen R H 1978, Phys. Rev. B **17**, 3710

Teitel S and Jayaprakash C 1983a, Phys. Rev. Lett. **51**, 1999

Teitel S and Jayaprakash 1983b, Phys. Rev. B **27**, 598

Tinkham M, Abraham D W and Lobb C J 1983, Phys. Rev. B **28**, 6578

Tinkham M 1975, *Introduction to Superconductivity* (McGraw-Hill, New York)

Villain J 1975, J. Phys. (Paris) **36**, 581

Villain J 1977, J. Phys. C **10**, 1717

Voss R F and Webb R A 1982, Phys. Rev. B **25**, 3446

Webb R A, Voss R F, Grinstein G and Horn P M 1983, Phys. Rev. Lett. **51**, 690

Yosefin M and Domany E 1985, Phys. Rev. B **32**, 1778

Young A P 1978, J. Phys. C **11**, L453